8-2014

Mitigation of Alkali-Silica Reaction (ASR) in an Interstate Median Barrier

Richard Albert Deschenes
University of Arkansas, Fayetteville

Mitigation of Alkali-Silica Reaction (ASR) in an Interstate Median Barrier

Mitigation of Alkali-Silica Reaction (ASR) in an
Interstate Median Barrier

A thesis submitted in partial fulfillment
of the requirements for the degree of
Master of Science in Civil Engineering

By

Richard Deschenes
University of Arkansas
Bachelor of Science in Civil Engineering, 2008

August 2014
University of Arkansas

This thesis is approved for recommendation to the Graduate Council.

Dr. W. Micah Hale
Thesis Director

Dr. Ernie Heysmfield
Committee Member

Dr. Clinton Wood
Committee Member

Abstract

In 2012 it was discovered that roughly 4 miles of interstate median barrier along Interstate 540 had rapidly deteriorated. After the initial inspection, a sample was submitted for analysis, and found to contain evidence of alkali-silica reaction (ASR). A research program was implemented with the goal of determining the cause of ASR and developing a program for mitigating the ongoing deterioration. The median barrier had not deteriorated equally throughout the 4 miles, and the level of damage varied considerable throughout the length. A visual inspection of the median barrier was conducted and the median barrier was divided into sections based on visible damage.

A research program was implemented to evaluate several treatment methods, with the goal of slowing or arresting the deterioration within the median barrier. Several sections of the median barrier were instrumented with devices to measure expansion and internal relative humidity. The sections were then treated and monitored to evaluate the efficacy of each treatment. The treatments were applied to sections of each damage level to evaluate the effect of damage at the time of treatment on the efficacy of the treatment. Monitoring was conducted for one year and some preliminary conclusions and recommendations were developed from the results.

The aggregates used in the median barrier construction were also evaluated in laboratory testing, which included the accelerated mortar bar test and the concrete prism test. The fine aggregate and course aggregate were evaluated, and the results compared to the findings from the petrographic analysis. Additionally the cement alkalis and supplementary cementations materials (SCMs) were evaluated to determine if they were a contributing factor in the development of ASR in the median barrier. The results of laboratory testing were used to develop recommendation on the prevention of ASR in concrete which contains these aggregates.

Acknowledgments

I would like to thank Dr. Micah Hale who inspired me to continue my education and who provided me with invaluable advice and support. I never imagined I could spend several years studying such a small aspect of the field of concrete materials. However, Dr. Hale's enthusiasm for research, and especially for teaching and advising, has inspired me to dedicate much time toward pursuing the dream of one day passing the knowledge of civil engineering and concrete materials on to another generation of engineers. Thank you for patiently encouraging me to work harder than I imagined possible and to see my dreams come to realization.

I must also thank the many students who have made my research possible. Cameron Murray's help was instrumental in the success of our research. Every time I needed help with instrumenting or measurements, Cameron was always available and always made his schedule work. Thank you for the help, advice, and support which was much needed in completing this research project. Casey Jones also assisted with the implementation of our research and was always willing to help out. Thanks also to William Philips, Doddridge Davis, and Cahn Dang for helping with the numerous measurement and instrumentation visits, and for being available whenever help was needed.

Thank you to all the faculty members of the University of Arkansas, Department of Civil Engineering who have had me in class. Thank you for the valuable knowledge, advice, and skills which you have passed on to me.

Dedication

This thesis is dedicated to my family. You have supported me throughout my life and college career, and have encouraged me to continue my education and to do more than I imagined possible. Thank you for continuing to support and encourage me in the pursuit of my dreams. And thank you for continuing to provide guidance, advice, and prayer when I am distracted or discouraged.

Table of Contents

List of Tables

List of Figures

1 Introduction and Background

During a 2012 visual inspection, premature deterioration of the Interstate 540 concrete median barrier and pavement was detected. A petrographic examination of concrete samples from the median barrier was conducted by Construction Technologies Laboratory Group (CTLGroup). In addition, two core samples were removed from the adjacent concrete pavement and sent for petrographic examination. The concrete from both the median barrier and interstate pavement were placed in 1998, and utilized the same aggregate and cement suppliers. Specimens from both concrete mixtures contained evidence of alkali-silica reaction (ASR) products. In addition, the deterioration was exacerbated by freezing and thawing action.

A research program began in May 2012 with the goals of determining the source of reactivity, developing preventative measures against ASR, and mitigating ASR in the median barrier and pavement. Laboratory testing to determine the source of reactive aggregates was conducted between July 2012 and January 2014. A method for mitigation was developed and implemented in January 2013, and field monitoring was conducted through January 2014. In addition, an extensive literature review was conducted to determine methods of mitigation and prevention which have been successful in similar situations.

The preliminary findings from laboratory research and field monitoring are presented herein. At this time only one year of field monitoring results are available. From the results, preliminary conclusions and recommendations are provided. However, a minimum of three years of monitoring is recommended to establish long term trends for the efficacy of mitigation methods. At this time recommendations are provided on the prevention of ASR in concrete through the use of low alkali cement and Class C fly ash. Some recommendations from the implementation of the field monitoring program are also provided.

1.1 Literature Review

1.1.1 Discovery

Stanton (1940) was the first to investigate ASR after several concrete structures in California developed premature deterioration, which was not attributed to any known durability issue at the time. Stanton (1940) determined that mortar bars, which contained high alkali cement and siliceous aggregates, produced deleterious expansion when exposed to damp conditions for over one year (Stanton, 1940; ACI, 1998). In addition Stanton's work provided the first test method for the evaluation of the expansive reaction between cement and aggregates (ACI, 1998). Stanton (1940) provided recommendations to prevent ASR, such as limiting the cement alkali content to 0.6 percent and/or replacing a portion of the cement with a supplementary cementitious material (SCM) (ACI, 1998).

1.1.2 Alkali-Silica Reaction (ASR)

When reactive siliceous minerals, from the aggregate, react with highly alkaline cement pore solution, ASR occurs (ACI, 1998; Diamond, 1989). The presence of sodium (Na), potassium (K), and other alkalis within the pore solution produces a very high equilibrium pH (Diamond, 1989). Reactive silica minerals dissolve when exposed to the high pH cement pore solution, and when sufficient calcium hydroxide is available, expansive alkali-silica gel will precipitate from the dissolved silica and alkali solution (Diamond, 1989). Once alkali-silica gel deposits form, the gel will imbibe water from the surrounding cement pore solution and expand (Powers & Steinour, 1955; Diamond, 1989). It is important to note that, depending on the availability of calcium hydroxide within the cement pore solution, not all alkali-silica gels are expansive (Powers & Steinour, 1955; Diamond, 1989; Helmuth, Stark, Diamond, & Moranville-Regourd,

1993). As the gel continues to adsorb water, the gel will produce an expansive pressure on the surrounding cement matrix and aggregates. The pressure is often sufficient to form microcracks within the cement matrix. In addition, as the reactive aggregate particles are eroded, and gel deposits form within the aggregate, the microcracks will extend into the aggregate particles. The micro-cracks will continue to expand until visible cracks develop (Diamond, 1989).

As stated, four components are required for ASR and expansion to occur within concrete (ACI, 1998; Stark, Morgan, Okamoto, & Diamond, 1993). The necessary conditions for expansive ASR to develop are shown in Figure 1.1. Reactive silica within the aggregate is necessary for the development of alkali-silica gel. Also, a high concentration of alkalis is necessary to produce the high pH within the cement pore solution. A limited amount of mobile Calcium hydroxide, within the cement pore solution, is required for expansive gels to precipitate (Diamond, 1989). Additionally, sufficient moisture is required for alkali-silica gel expansion to occur and continue (ACI, 1998).

Reactive siliceous minerals are present within many coarse and fine aggregates. Some common siliceous minerals include: opal, chalcedony, quartz, cristobalite, tridymite, volcanic glasses, and chert (ACI, 1998; Helmuth et al., 1993). Reactive siliceous minerals have a disordered crystal structure which may react and dissolve when exposed to a highly alkaline cement pore solution (Powers & Steinour, 1955; Helmuth et al., 1993). However, not all minerals have the same level of disorder within the silica crystals. Therefore, disordered minerals such as opal will react much faster than ordered minerals such as quartz. As the concentration of alkalis within the cement pore solution increases, the silica minerals are dissolved faster and more expansion occurs (Powers & Steinour, 1955; Helmuth et al., 1993).

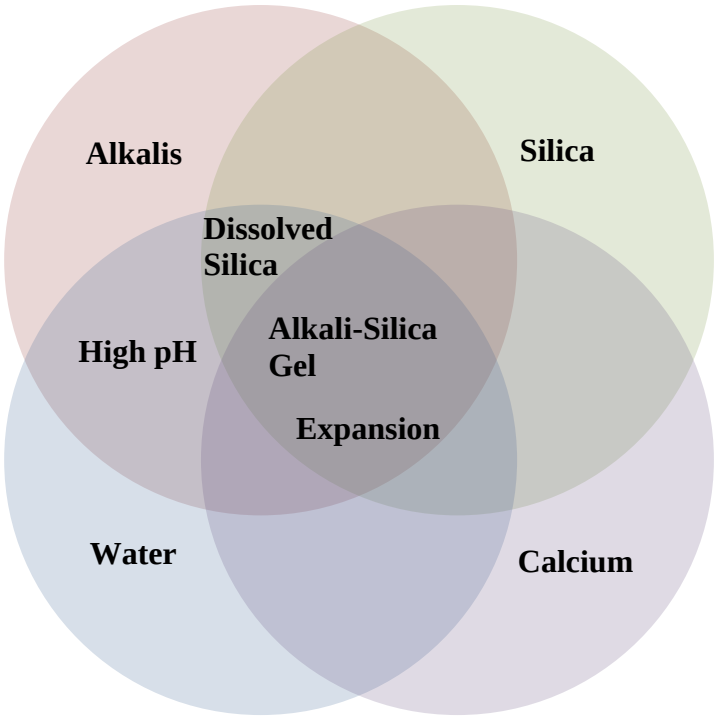

Figure 1.1. Components required for alkali-silica gel to develop and expand.

1.1.2.1 Alkalis and Calcium

Soluble alkalis including sodium hydroxide (NaOH) and potassium hydroxide (KOH) are released into the cement pore solution during hydration (Helmuth et al., 1993). As hydration continues some of the alkalis are used up in the reaction products; however, the water is also used up and the alkali concentration increases (Powers & Steinour, 1955; Diamond, 1989). Diamond (1989) discovered a linear relationship between alkali concentration in cement pore solution and the available alkali content of the cement (Helmuth et al., 1993). As the available alkalis within the cement increases, the concentration of alkalis within the pore solution of the concrete increases. Powers & Steinour (1955) stated the importance of calcium in the formation of expansive alkali-silica gels. When excess calcium hydroxide is available within the alkali-silica gel, the gel is unstable and produces dissolved silica which will not expand. However, when the calcium-alkali-silica system produces a barrier to the transport of excess calcium to the

reaction site, a stable alkali-silica gel is produced which then adsorbs water and expands (Powers & Steinour, 1955; Helmuth et al., 1993). The process of dissolving silica minerals in the presence of highly alkaline pore solution will continue until either all of the reactive silica or all of the alkalis are consumed (Helmuth et al., 1993).

1.1.2.2 Expansion and Moisture

ASR is a two phase deleterious reaction (Diamond, 1989; Helmuth et al., 1993). The first phase described above involves the precipitation of expansive alkali-silica gel during the reaction between highly alkaline cement pore solutions and reactive siliceous minerals (Diamond, 1989). The second phase involves the adsorption of water into the alkali-silica gel, which produces expansion and pressure (Diamond, 1989; Helmuth et al., 1993). The alkali-silica gel is insoluble and acts as a membrane between the gel material and cement pore solution (Powers & Steinour, 1955; Diamond, 1989). Pore solution is drawn, by the reduced free energy within the alkali-silica gel, through this membrane into the alkali-silica gel and produces expansion (Powers & Steinour, 1955; Diamond, 1989; Helmuth et al., 1993). However, the expansion is limited by the availability of moisture to the expansive gel (Stark, 1990; Fournier, Bérubé, Thoma, Smaoui, & Folliard, 2004). Stark (1990) reported a limiting value of 80 percent internal relative humidity, at a reference temperature of 21 to 24 degrees Celsius, which is required for expansion to continue.

1.1.3 Diagnosing ASR

The symptoms of ASR are similar to other durability mechanisms which occur in concrete (Fournier et al., 2004). Some of the visible symptoms of ASR include map cracking at the surface of the concrete or relative displacement of concrete elements (Stark 1991; Fournier,

Bérubé, Folliard, & Thomas, 2010; ACI, 1998; Fournier et al., 2004). Additional symptoms include pop-outs, surface discoloration, and/or gel exudation at the surface (Stark, 1991; Fournier et al., 2010; ACI, 1998; Fournier et al., 2004). Often the concrete is discolored along cracks, especially when the concrete is moist (Stark, 1991; Fournier et al., 2010; and ACI, 1998). Some typical symptoms of ASR are shown in Figure 1.2. Expansion greater than 0.04 percent will lead to visible cracking in unreinforced concrete (Ideker, Bentivegna, Folliard, & Juenger, 2012a).

Figure 1.2. Example of ASR symptoms such as map cracking, cracks parallel to restraint, gel exudation, and surface discoloration. Picture used with permission from Richard Deschenes.

Map cracking occurs in concrete elements which are subjected to cyclic environmental conditions. The concrete within an element will expand more than the outer surface due to a temperature and humidity gradient which develops between the surface and interior concrete (Fournier et al., 2004). As shown in Figure 1.3, expansion of the concrete will produce tensile stresses and micro-cracks in the interior concrete, and drying shrinkage near the surface will cause map cracking in the exposed surfaces of the concrete (ACI, 1998; Fournier & Bérubé, 2000; Fournier et al., 2004).

Concrete with anisotropic restraint, either by internal reinforcement or adjacent concrete members, will develop cracks parallel to the primary restraint (Stark, 1991; Fournier et al.,

2004). Unfortunately, it is not possible to diagnose ASR with visual symptoms alone, because other durability problems such as freezing and thawing, corrosion, sulfate attack, and shrinkage exhibit similar symptoms (Thomas, Fournier, Folliard, & Resendez, 2011; ACI, 1998). Therefore petrographic examination of the concrete is required to diagnose the presence of ASR (Stark, 1991; ACI, 1998).

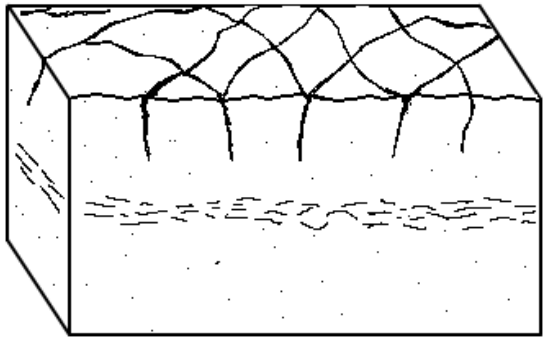

Figure 1.3. Concrete element showing map cracking at the surface and microcracks parallel to the surface, due to the humidity gradient between the exposed surface and the internal concrete. Picture recreated from ACI (1998).

1.1.3.1 Petrographic Examination

Conclusive evidence of ASR is found in concrete only though petrographic examination. The examination includes both microscopic and macroscopic identification of symptoms of ASR. Macroscopic evidence of ASR includes deposits of alkali-silica gel which are identified visually and chemically (Fournier et al., 2004; ACI, 1998). Deposits of alkali-silica gel develop within voids in the cement pore solution and within cracked aggregate particles (Fournier et al., 2004; Fournier et al., 2010). Additionally, reaction rims are sometimes present within the interfacial transition zone around reactive aggregate particles (Fournier et al., 2004; Fournier et al., 2010; ACI, 1998). Microscopic evidence of ASR may include micro-cracking within aggregates and/or the cement matrix, reaction rims, and alkali-silica gel (Fournier et al., 2004; Fournier et

al., 2010). Petrographic examination is necessary to provide a conclusive diagnosis of the presence of ASR and other forms of deterioration that may have occurred as a result of, or in combination to, ASR (Fournier et al., 2004; ACI, 1998; Fournier et al., 2010).

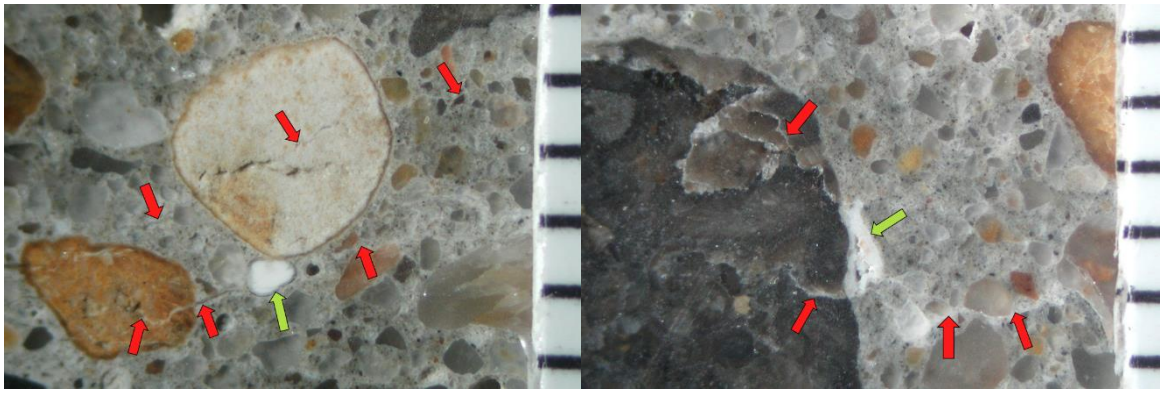

Figure 1.4. Typical petrographic features, including micocracking within fine aggregate particles and extending into the cement matrix (red arrows) and alkali-silica gel deposits (green arrow). Pictures from CTLGroup (2012).

1.1.4 Prevention of ASR

Several options are available for the prevention of ASR in concrete. The most effective method for the prevention of ASR involves controlling one or more of the three constituents required for ASR to develop (ACI, 1998). Moisture is required for ASR to develop and expansion to progress; however, limiting water is a prohibitive method of preventing ASR. The most common method of prevention involves limiting the concrete pore solution alkalinity (ACI, 1998). Cement alkalis are most readily available within the cement pore solution (Diamond, 1989; Thomas, 1995). However, alkalis are sometimes contributed by SCMs or even aggregates (ACI, 1998; Thomas, 1995). The use of low alkali cements will reduce cement pore solutions alkalinity, and a limit of 0.6 percent Na_2O_e is recommended when used in combination with reactive aggregates (Thomas, Fournier, Folliard, Ideker, & Shehata, 2006a; ACI, 1998; Stanton, 1940). However, in certain highly reactive aggregates this limit is not sufficient (Stark, 1980;

ACI, 1998; Swamy & Al-Asali, 1988b). In addition, SCMs dilute high alkali cements or bind the available alkalis within the hydration products (ACI, 1998). Some of the SCMs which prevent or reduce ASR expansion include slag cement, fly ash, calcined clays, rice husk ash, and silica fume (ACI, 1998; Thomas et al., 2006a). The safe replacement rate of cement with an SCM will depend on the cement alkalis, aggregate reactivity, selected SCM, and chemical and physical composition of the SCM (ACI, 1998; Thomas et al., 2006a; Thomas, 1995).

1.1.4.1 SCM mechanisms

The mechanisms by which SCMs prevent ASR depend on the SCM, the compositions of the SCM, and the level of replacement (ACI, 1998; Thomas, 1995). The first mechanism involves decreasing cement alkalis, by replacing a portion of the cement with a lower alkali SCM (ACI, 1998; Thomas, 1995). The second mechanism involves the production of secondary calcium silicate hydrates which bind alkalis and reduce the pore solution alkalinity (ACI, 1998; Thomas, 1995; Duchesne & Berube, 1994). Additionally, the pozzolanic reaction can consume calcium hydroxide and reduce the expansion of ASR gel (ACI, 1998; Thomas, 1995; Duchesne & Berube, 1994). Finally, the improved production of calcium silicates produces lower permeability and reduces the mobility of alkalis (ACI, 1998; Thomas, 1995).

The efficacy of an SCM also varies with the composition of the particular SCM. The lime content of fly ash depends on the coal used in the production of the fly ash. Class C ashes contain 8 percent or more lime, and are both cementitious and pozzolanic. The cementitious properties of Class C ashes releases additional alkalis and makes Class C ashes less effective at preventing ASR; therefore, a replacement rate of 40 to 50 present is required (ACI, 1998; Shehata & Thomas, 2000; Thomas, 1995). Class F fly ashes contain less than 8 percent lime and

are purely pozzolanic, the improved production of calcium silicates produces a reduction in ASR expansion with replacement rates between 15 and 30 percent (ACI, 1998; Shehata & Thomas, 2000). Slag cement is also used to prevent ASR expansion; however, at replacement rates between 25 and 50 percent (ACI, 1998; Thomas, 1995). The higher replacement rates are required because the alkalis within the slag cement are released into the pore solution and require additional secondary hydration to bind and dilute the alkalis (ACI, 1998; Thomas, 1995).

An additional option for the prevention of ASR is lithium nitrate, which is added to concrete mixtures and will prevent the development of expansive alkali-silica gel (Thomas et al., 2006a; Folliard, Barborak, Ideker, Fournier, & Thomas, 2007). The required dosage of lithium is determined through accelerated testing (Folliard et al., 2007).

1.1.5 Test Methods for Assessing Alkali-Silica Reactivity

Several laboratory test methods exist which can determine the alkali-silica reactive potential of aggregates or aggregate and cement combinations. The first test method was developed by Stanton (1940) and involved producing mortar bars with the selected aggregate and cement (ACI, 1998; Stanton, 1943). The mortar bars were stored in moist conditions within sealed containers for up to two years, with expansion measured periodically. The test method was similar to the ASTM C227 mortar-bar test which was developed in the 1950's (ACI, 1998; Thomas et al., 2006a). The mortar bar test method was useful for evaluating reactive aggregates; however, the test had several limitations. The mortar-bar test method was susceptible to alkali leaching due to the transport of alkalis through water which precipitated on the surface of the mortar bar (Stanton, 1943; Thomas et al., 2006a; ACI, 1998; Rogers & Hooton, 1991). In addition, the mortar bar test duration was one year and did not accurately access slowly reactive

aggregates. Therefore, Davies and Oberholster (1986) developed an accelerated mortar bar test (AMBT) method, based on recommendations originally made by Stanton (1943). The AMBT evaluated the expansion of reactive aggregates in only 16 days. The AMBT could also detect expansion in slowly reactive aggregates, and was not susceptible to alkali leaching due to the additional alkalis provided by the NaOH soak solution (ACI, 1998; Thomas et al., 2006a).

1.1.5.1 Accelerated Mortar Bar Test (AMBT)

The AMBT is similar to the mortar-bar test, with a modified storage environment. The mortar bars are one 25 mm (1 in.) square and 285 mm (11.25 in.) long, with stainless steel gage studs attached at the ends for length comparator readings. The aggregate gradation is standardized to improve repeatability. Coarse aggregates are crushed and sieved to match the gradation. However, crushing the aggregate potentially changes the reactivity of the aggregate (Du-you, Fournier, & Grattan-Bellew, 2004). The mortar bars are stored in 1 N NaOH solution to prevent alkali leaching, and at 80 degrees Celsius to accelerate expansion (ACI, 1998; Rogers & Hooton, 1991). Davies and Oberholster (1988) conducted testing on the mechanism and reaction products of alkali-silica gel within AMBT specimens, and concluded that the mechanism and reaction products were not altered by the accelerated conditions (Davies & Oberholster, 1988). The duration of the AMBT is 16 days, which includes one day of curing, an additional day of storage in water at 80 degrees Celsius, and then 14 days stored at 80 degrees Celsius in NaOH (ACI, 1998; Thomas et al., 2006a; Ideker et al., 2012a; ASTM, 2008a). Due to the alkali solution used in storage, the cement alkali used for testing has little effect on the final expansion (Du-you et al., 2004).The AMBT was standardized under ASTM C1260 and is used to screen aggregates for potentially deleterious expansion (ASTM, 2008a). Due to the harsh environment in which the mortar-bars are stored, the AMBT method often falsely assesses aggregates as

reactive, which exhibit good field performance in concrete (Thomas et al., 2006a; Ideker et al., 2012a; Touma, Fowler, Carrasquillo, Folliard, & Nelson, 2001). Therefore, additional test methods, such as the concrete prism test (CPT), are conducted for aggregates which develop potentially deleterious expansion during AMBT testing (Thomas et al., 2006a; Ideker et al., 2012a; Fournier, Bérubé, & Frenette, 2000). Although the AMBT has been standardized, there is some disagreement about the final expansion which indicates reactive aggregates. Generally, expansion greater than 0.10 percent at 14 days indicates a potentially expansive aggregate (Fournier el al., 2000). However, some authors have recommended lowering this limit to 0.08 percent for slowly reactive aggregates (Stark et al., 1993; ACI, 1998).

The AMBT is also applicable when assessing the safe replacement rate of SCMs for the prevention of ASR in mortars with known reactive aggregates (Fournier et al., 2000; Thomas et al., 2006a). A specification was developed for this purpose and standardized as ASTM C1567 (ASTM, 2008b). The test method is similar to the AMBT, with the exception of the cementitious materials. A portion of the cement is replaced with the selected SCM, and the test duration extended to 28 days (Touma, 2000). The test method provides conservative replacement rates for SCMs when preventing ASR in concrete is required. However the test method is not applicable when evaluating safe cement alkali levels (Thomas et al., 2006a). The two-year CPT is more reliable when evaluating reactive aggregates and safe SCM replacement rates (Thomas, Fournier, & Folliard, 2008).

1.1.5.2 Concrete Prism Test (CPT)

The AMBT has several limitations which prevent the test from producing reliable results for certain aggregates. In addition, the AMBT is only applicable to evaluate aggregates in mortar

samples. Expansion produced in AMBT mortar bars does not correlate to expansion developed in the field (Ideker et al., 2012a). The concrete prism test (CPT) was developed to more accurately predict the expansion of concrete containing reactive aggregates (ACI, 1998; Ideker et al., 2012a). The CPT is standardized under ASTM C1293 (ASTM, 2012). The CPT specifies the coarse aggregate gradation, cement content, and water to cement ratio (ACI, 1998; ASTM, 2012). The cement alkali content is limited to 0.90 ± 0.1 percent. However, the alkalis are increased to 1.25 percent through the addition of NaOH to the mixing water (ACI, 1998; Thomas et al., 2006a; ASTM, 2012). The test duration is one year, and the specimens are stored in a sealed container over water at a constant temperature of 38 degrees Celsius, and relative humidity greater than 95 percent (ASTM, 2012).

The concrete prism test is highly susceptible to alkali leaching and a wicking material is required within the storage container to prevent moisture from precipitating on the surface of the prisms (Rogers & Hooton, 1991; Thomas et al., 2006a; Ideker et al., 2012a). The limitations of the CPT include the relatively long, one-year, test duration and the effects of alkali leaching (ACI, 1998; Thomas et al., 2006a). In addition, because alkalis are increased to 1.25 percent, the test is not applicable when evaluating the safe cement alkali level of a concrete mixture (Thomas et al., 2006a). The two-year CPT is the most accurate accelerated method for assessing the potential for deleterious expansion in concrete, and for determining safe replacement rates of SCMs (Ideker et al., 2012a; Ideker et al., 2012b; Touma et al., 2001; Fournier et al., 2000). Fournier et al. (2000) recommended evaluating the field combination of fine and coarse aggregates together, and extending the test duration to two year.

1.1.5.3 Outdoor Exposure Block Test

Due to the limitations within accelerated laboratory test methods, field service records are often the best method for determining the long term performance for a concrete mixture (Thomas et al., 2006b; Ideker et al., 2012a; Ideker et al., 2012b). One method of measuring field performance under controlled conditions is the large block exposure site test. One advantage of the large block test is the ability to evaluate a concrete mixture in field conditions. Additionally, the concrete mixture may contain cements with any alkali level, and any combination of SCMs (Thomas et al., 2006b; Ideker et al., 2012b). Expansion is monitored using detachable mechanical (DEMEC) type strain gages in combination with gage studs affixed to the surface of the blocks. Alternately, vibrating-wire strain gages are embedded within the concrete during placement, with the advantage of continuous expansion monitoring. Internal relative humidity and temperature are monitored with hand-held instruments and probes, which are inserted into holes, drilled in the block. Several outdoor exposure sites have been constructed in the United Kingdom, Canada, and the United States (Thomas et al., 2006a; Ideker et al., 2012b; Thomas et al., 2006b).

Although there are no standards available for the large block exposure site test, recommendations are available in the literature. The size of blocks range from 350 mm to 900 mm, although some blocks are as large as 3 m (Ideker et al., 2012b; Thomas et al., 2006a). Researchers at the International Center for Aggregate Research (ICAR) recommend blocks with dimensions of 380 x 380 x 710 mm (Ideker et al., 2012b; Folliard et al., 2012). Cement alkalis are increased to 1.25 percent Na_2O_e when evaluating mitigation measures. However, low alkali cement mixtures are evaluated without increased alkalis (Ideker et al., 2012b). The coarse aggregate volume fraction

is the same as used in the CPT; however, it is also possible to evaluate the natural gradation (Ideker et al., 2012b; Folliard et al., 2012).

The outdoor exposure site test is considered the most accurate method of measuring field performance of concrete mixtures. The test method is often used to validate the results of accelerated laboratory test methods. The ambient conditions vary with the region where the site is constructed, and best represent the conditions which the concrete is subjected to in the field (Ideker et al., 2012b). The major limitation of the outdoor exposure site test is the extended time required to produce results, which is greater than 10 years when evaluating field performance (Ideker et al., 2012b). However, the test can produce results on preventative measures and mitigation methods in less time.

1.1.6 Test Methods for ASR in Existing Concrete Elements

In structures which exhibit ASR symptoms, it is often necessary to monitor the progression of damage and, if applicable, to monitor the effectiveness of mitigation methods (Fournier et al., 2004). Damage is measured through a combination of in-situ measurements, which may include destructive and/or non-destructive methods. The most common destructive method involves removing core samples for analysis. Core samples are then used for various tests including petrographic analysis, concrete mechanical properties tests, or quantitative damage indices (e.g. Damage Rating Index). An additional test method involves subjecting cores to accelerating conditions (similar to the AMBT or CPT) to determine the potential for future expansion, which is then used in conjunction with in-situ expansion data to evaluate the current state of a concrete element and to develop treatments and retrofits as they become necessary (Fournier et al., 2004).

Petrographic examination is an important step in diagnosing the presence of ASR and/or other deterioration mechanisms within concrete. Core samples are extracted from the concrete element and then visually inspected for symptoms of ASR. Some symptoms which are identified under the microscope include microcracks, reaction products (ASR gel), reaction rims, and changes in the interfacial transition zone (Fournier et al., 2004). Before these symptoms are identified, the concrete sample is polished or cut into thin sections and analyzed under a low powered microscope (Fournier et al., 2004). Additionally, damage indices are used to quantify and compare the petrographic features of ASR (Fournier et al., 2004). The damage rating index (DRI) is a quantitative measure of several petrographic features and is useful for comparing the progression of ASR damage in concrete over time, or between separate concrete elements within a structure (Smaoui, Berube, Fournier, Bissonnette, & Durand, 2004; Shrimer, 2000).

Mechanical tests of core samples are useful when evaluating the loss of engineering properties within concrete affected by ASR (Fournier et al., 2004). Compressive and tensile strength tests of core samples are used to determine the loss of strength within a concrete element due to ASR deterioration (Fournier et al., 2004). Tensile strength deteriorates much more rapidly than compressive strength during ASR expansion and is a better indicator of the level of damage (Fournier et al., 2004; Swamy & Al-Asali, 1988a). The stiffness Damage Index was developed as a method of estimating the expansion-to-date within a concrete element. The test method involves subjecting a core to five cycles of loading and unloading, and measuring the plastic deformation and energy dissipation (Fournier et al., 2004; Smaoui et al., 2004).

A more common test involves subjecting cores to expansion accelerating conditions to estimate the potential for future expansion (Fournier et al., 2004; Fournier et al., 2010). Two cores are required for this method, the first core is subjected to the same conditions as the CPT (38 degrees

C and 95 percent RH) and the expansion is monitored to assess the degree of future expansion. The second core is submerged in 1N NaOH at 38 degrees Celsius and the expansion monitored to determine the absolute degree of reactivity of the aggregates within the concrete (Fournier et al., 2004; Fournier et al., 2010).

The destructive test methods provide some insight into the future expansion and deterioration which will occur in the concrete. These methods in addition to in-situ monitoring are used to develop a plan of mitigation and/or remediation which will extend the useful life of the concrete element.

1.1.6.1 In-situ (Field) Monitoring

In-situ expansion monitoring is used to determine the expansion rates and potential of concrete structures (Fournier et al., 2004; Fournier et al., 2010; Drimalas, Folliard, Thomas, Fournier, & Bentivegna, 2012; Thomas, Folliard, Fournier, Drimalas, & Rivard, 2012). Reference gage studs are affixed to the concrete. The gage studs have a small machined indent which is matched up with the points on a DEMEC gage. Periodic measurements are then taken between two gage studs to monitor the progression of expansion along an axis of the concrete element (Fournier et al., 2004; Fournier et al., 2010). Vibrating wire strain gages have also been used successfully to monitor expansion continuously, with the ability to transmit measurements automatically (Fournier et al., 2004).

Another important characteristic to monitor is the change in internal relative humidity and temperature. Portable humidity probes are available which are inserted into holes drilled into the concrete element, and report the internal temperature and relative humidity (Fournier et al., 2004; Fournier et al., 2010; Thomas et al., 2012). However, the probe must remain in the concrete

until equilibrium is reached between the air in the hole and the moisture in the cement pore solution. The internal relative humidity is monitored to determine the effectiveness of a mitigation method. If the internal relative humidity is reduced below 80 percent, referenced to 21 degrees Celsius, ASR will arrest (ACI, 1998; Stark, 1990).

1.1.7 Mitigation of ASR

Although there are several effective methods for the preventing of ASR, concrete structures which develop ASR are still constructed. Mitigating ASR in hardened concrete is much more prohibitive than preventing ASR in fresh concrete. Several repair or rehabilitation methods are available for various concrete structures (ACI, 1998; Fournier et al., 2004). Transportation structures such as pavements, bridge decks and elements, and median barriers often have large surface areas compared to volume. In structures with relatively thin cross sections, and high surface area to volume ratios, controlling internal moisture is often the best method of mitigating ASR (ACI 1998, Fournier et al., 2004). As stated earlier, an internal relative humidity greater than 80 percent will cause expansion to continue (ACI, 1998; Stark, 1990). In some concrete elements protection from rain or groundwater is possible, and will reduce expansion. The most promising method of moisture protection for bridge elements and median barriers has been silane (ACI, 1998; Berube et al., 2002b; Drimalas et al., 2012; Thomas et al., 2012; Fournier et al., 2004). However, there is very little published literature on the long term efficacy of silane on concrete pavements.

Abundant literature has been published on the efficacy of topical lithium treatment used to mitigate ASR. If a sufficient dose of lithium is introduced into the concrete pore solution, ASR expansion will cease (Folliard et al., 2007; Stark et al., 1993). However, due to the low

permeability of hardened concrete, it is difficult to introduce the required dose of lithium through the full depth of a concrete element (Johnston, Surdahl, & Stokes, 2000; Folliard et al., 2012; Tuan, Kelly, Sun, & Buss, 2005). Several methods have been used to increase the penetration of lithium into concrete structures, with limited success (Stokes, Pappas, Thomas, & Folliard, 2002; Thomas et al., 2012; Drimalas et al., 2012). Concrete elements treated topically, through vacuum impregnation, or electrochemical impregnation with lithium nitrate produced varying levels of penetration depending on the level of concrete cracking at the time of treatment (Stokes et al., 2002; Johnston et al., 2000). However, even in moderately cracked element, the penetration depth for a sufficient dose of lithium within the cement pore solution was only 50 mm (Stokes et al., 2002; Johnston et al., 2000; Folliard et al., 2012).

Topical applications of breathable vapor barriers have proven more effective in reducing ASR expansion in some concrete elements. Topical application of silane or siloxane can reduce internal relative humidity within thin concrete elements for 5 or more years (Berube et al., 2002b). Additional researchers included elastomeric paint crack bridging surface treatments to control internal humidity in concrete with wide cracks (Drimalas et al., 2012; Thomas et al., 2012; Fournier et al., 2004).

1.1.7.1 Stark et al. (1993)

The mitigation of ASR in concrete pavements is mentioned by Stark et al. (1993), in a study of concrete bridge decks and pavements. The monitoring program consisted of falling weight deflectometer (FWD) and internal relative humidity measurements (Stark et al., 1993). Internal relative humidity was monitored through a method developed by Stark (1990) in which powder concrete samples were removed by drilling into the concrete and collecting samples at selected

depths within the concrete (Stark et al., 1993). The samples were then stored in a bottle and the equilibrium relative humidity within the bottle was measured with a probe (Stark et al., 1993). Samples from various depths were then assembled to produce a relative humidity gradient with respect to depth of concrete (Stark et al., 1993). Deflection measurements were taken before treatment and then again one year after treatment (Stark et al., 1993). These measurements were then correlated to elastic modulus of the concrete, and used to monitor the progression of ASR within the concrete (Stark et al., 1993). The surface treatments evaluated in the study included lithium, silane, and linseed oil. Unfortunately, only one year of monitoring was provided, and no conclusions were made on the effectiveness of the sealers (Stark et al., 1993). However, Stark et al. (1993) did conclude that FWD was a valid method of monitoring the deterioration of pavements due to ASR.

Stark et al. (1993) reported that silane treatment of concrete pavements only provided a reduction in internal relative humidity within the top 0.5 to 1 inch of pavement. Stark et al. (1993) postulated that the silane was ineffective at mitigating expansion in concrete pavements due to moisture moving into the pavement from the subgrade. However, only one year of monitoring was available to develop this conclusion, which is not long enough to provide conclusive results on the efficacy of a surface treatment. The report also determined that topical lithium produced the greatest reduction in expansion, again from one year of monitoring. Several publications have reported that the penetration of lithium into hardened concrete was not sufficient to provide a beneficial reduction in expansion (Stokes et al., 2002; Johnston et al., 2000; Folliard et al., 2012). More recent publications on the efficacy of topical silane mitigation in concrete transportation structures agree that silane provides a reduction in internal relative humidity

(Bérubé et al., 2002a; Drimalas et al., 2012; Thomas et al., 2012). However, none of these publications specifically address concrete pavements treated with silane.

1.1.7.2 Berube et al. (2002a)

Berube et al. (2002a) provided conclusive results on the efficacy of silane and siloxane sealers from over 10 years of expansion and internal relative humidity monitoring of median barriers. The monitoring program involved selecting sections for treatment and control and then instrumenting the sections with expansion monitoring grids and internal relative humidity and temperature probes (Berube et al., 2002a). Gage reference studs were affixed to the wall, with drilled points in the gage reference studs which were matched up with the points on the ends of a detachable mechanical strain (DEMEC) gage. The length-change between two gage reference studs was then used to monitor expansion. Gage reference studs were positioned for vertical and thickness length-change measurements. In addition holes were drilled in each section to monitor internal relative humidity and temperature with a commercial humidity probe (Berube et al., 2002a). Results from 10 years of monitoring indicate that both silane and siloxane produce a reduction in expansion and internal relative humidity for treated sections as compared to the control (Berube et al., 2002a). The silane treatments were more effective than the siloxanes at reducing expansion. The treatments decreased internal relative humidity for 6 years, and then had reduced effectiveness (Berube et al., 2002a). Therefore, Berube et al. (2002a) recommends a reapplication of silane after 5 to 6 years of service. In addition, silane was effective in reducing expansion in moderately damaged median barriers for 10 years and 6 years, respectively. However, the siloxane treatment was less effective when used on severely damages sections, and only provided 1 to 2 years of protection (Berube et al., 2002a). These results are based on the

evaluation of concrete median barriers; however, they are applicable to concrete members with similar thickness and exposure conditions (Berube et al., 2002a).

1.1.7.3 Berube et al. (2002b)

Freezing and thawing cycles exacerbate the deterioration of damage in concrete which has cracked due to ASR (Berube et al., 2002a). However, treating the samples with silane, siloxane, or linseed oil can protect the concrete from moisture, and therefore expansion (Berube et al., 2002a). An extensive laboratory evaluation of the effectiveness of sealers on concrete samples affected with ASR and subjected to freezing and thawing cycles was conducted by Berube et al. (2002a). Samples treated with silane, siloxane, or linseed oil and subjected to freezing and thawing and ASR expansion in the laboratory exhibited a reduction in expansion as compared to untreated control samples (Berube et al., 2002a). A strong correlation between ASR expansion and internal relative humidity was also noted (Berube et al., 2002b). Silane showed the greatest ability to reduce expansion in concrete which had ASR and was subjected to freezing and thawing cycles (Berube et al., 2002b). The concrete sealed with linseed oil exhibited a reduction in expansion; however, the expansion still resulted in cracking when subjected to freezing and thawing (Berube et al., 2002b). The results showed that any reduction in expansion correlated to a reduction in moisture, and therefore humidity, within the concrete after it was sealed (Berube et al., 2002b).

1.1.7.4 Drimalas et al. (2012)

Several mitigation methods were evaluated under the FHWA Alkali-Silica Reactivity (ASR) Development and Deployment Program. Preliminary results from this program are summarized by Drimalas et al. (2012). The first mitigation evaluation involved several bridge columns in

Texas which had expansion due to ASR, and the second involved a median barrier in Massachusetts which also exhibited ASR (Drimalas et al., 2012). The column treatments included silane, or lithium applied through vacuum impregnation or electrochemical migration. The median barrier treatments included lithium, silane, penetrating membrane, and lithium vacuum impregnation (Drimalas et al., 2012). The columns treated with lithium did not develop sufficient penetration of lithium or a reduction in expansion. Silane produced the only reduction in expansion for both the columns and median barrier (Drimalas et al., 2012). As with all ASR field research, several years of monitoring are required to produce conclusive results. Both the columns and median barriers were monitored for 5 years; therefore, results on the sealer durability were not available. However, the results demonstrate the efficacy of silane in protecting concrete from moisture and reducing expansion.

1.1.7.5 Thomas et al. (2012)

Some additional research projects included under the FHWA Alkali-Silica Reactivity (ASR) Development and Deployment Program were reported by Thomas et al. (2012). These projects included a bridge structure in Maine, and a bridge in Vermont. Surface treatments evaluated in the study included silane or elastomeric paint (Thomas et al., 2012). Several columns were also treated with lithium nitrate through either vacuum or electrochemical impregnation, or with topical silane. The bridge in Maine was treated in 2009 and the bridge in Vermont was treated in 2010. Unfortunately, the study did not provide any preliminary results on the efficacy of the surface treatments.

These few case studies on the efficacy of surface treatment methods show promising results with methods such as silane, siloxane, and elastomeric paint. However, no conclusive case studies

were available on the efficacy of surface treatments applied to pavement structures. There is concern that moisture will enter the concrete pavement from the subgrade. Especially after treatment, when a humidity gradient is present within the concrete pavement. The humidity gradient may provide suction, and draw moisture out of the subgrade. In addition, the pavement is subject to traffic wear which may reduce the effective life of the treatment. Unfortunately, at this time, no conclusive long term results were published on the efficacy of surface treatments applied to pavements affected by ASR.

2 Materials and Methods

The research program was divided into three major phases. The first phase included an extensive review of available construction documents and records to determine and catalog the materials used in the concrete mixture within the median barrier. The information collected was then used in combination with the petrographic examination to determine the cause of the premature deterioration within the median barrier. The second phase involved a laboratory evaluation of the aggregates used within the concrete median barrier. The tests included the AMBT to evaluate the aggregates for potentially deleteriously reactive aggregates. The AMBT was followed by the CPT conducted on the aggregates to verify the results of AMBT and petrographic analysis. The final phase included instrumentation of the median barrier for length-change and internal relative humidity monitoring, followed by surface treatment and one year of monitoring to evaluate the efficacy of each treatment. The results of the three phases were compiled to evaluate methods for the prevention of ASR in concrete structures constructed with similar concrete mixtures that contain the same aggregates. The field investigation results were used to evaluate methods for mitigating ASR in concrete elements with varying degrees of surface cracking.

2.1 Preliminary Investigation

The preliminary investigation involved three stages which were conducted before the laboratory and field investigation. Severe surface deterioration along several sections of the median barrier was detected during scheduled maintenance. Due to the ambiguity of the symptoms of concrete durability issues, a petrographic analysis was required to determine the mechanisms by which severe expansion and cracks developed within the median barrier.

Visible surface cracking exist in all sections of the median barrier throughout the 4.4 mile length of the median barrier. However, the severity of the cracking varies between sections of the median barrier. To evaluate the variability in the degree of damage a visual inspection of the median barrier was conducted. The results of the visual inspection were used in selecting sections for the evaluation of treatments.

An effort was made to collect and review the construction documents and material records from the construction of the median barrier. Although some documents were available, much of the documents were destroyed, as there was no requirement to maintain records 10 years after construction. The records made available, were used in better understanding the variability in damage levels along the median barrier. Additionally, the records were utilized to locate original sources of materials, used in the median barrier concrete mixture, for laboratory testing.

2.1.1 Petrographic Analysis

When severe deterioration of the median barrier was detected in 2012, core samples were extracted and shipped to Construction Technologies Laboratories Group (GTLGroup) for petrographic examination. Due to practical limitations in conducting extensive petrographic examinations, only three samples were examined. The petrographic examination was performed in accordance with ASTM C856 Standard Practice for Petrographic Examination of Hardened Concrete. The evaluation included estimates of concrete properties and the source of the extensive cracking. The median barrier samples were first cut and polished, for examination with a stereomicroscope. A small section of the sample was then polished to produce thin-sections for polarized light microscopy.

The petrographic examination included an evaluation of the cement-paste and aggregates, followed by an evaluation of cracking and the mechanisms by which the cracks originated. The estimated concrete properties included water to cementitious material ratio (w/cm), air content and entrainment, calcium hydroxide content, non-hydrated cement content, and SCM content. The samples were also evaluated for secondary deposit (e.g. alkali-silica gel). Larger secondary deposits were evaluated in the polished section using a stereomicroscope, and the mineral composition of secondary deposits and reaction rims were observed in the thin-sections via polarized light microscopy. The aggregate mineral composition, gradation, texture, and distribution was also observed and classified. The presence of micro and/or macro cracks was observed visually and under stereomicroscopic magnification. The origination and progression of the cracks was noted and utilized in determining the mechanism of the crack formation.

The results of the petrographic examination were utilized in developing a system of laboratory investigation for the identification of reactive aggregates and an evaluation of the durability of concretes produced with reactive aggregates. The findings of the petrographic examination were verified through laboratory investigation of aggregates from the same source as those present within the concrete median barrier. The findings of the petrographic examination are discussed in Chapter 3.

2.1.2 Visual Inspection of Median Barrier

A visual inspection of the median barrier was necessary to locate sections with varying degrees of damage. Three damage levels were designated, and each median barrier section was classified as one of the three damage levels. Due to the length of the median barrier, an extensive evaluation was impracticable. However, a visual survey of the median barrier was possible if

broad categories of visual damage were determined. Therefore, three damage levels were selected to rapidly and accurately evaluate the median barrier sections. A typical 'section' of median barrier represents a length of 12 to 15 feet, a height of 3.5 feet, and the sections were divided at expansion joints.

The three damage levels were categorized as minimal, moderate, or severe damage. The minimal damage level included sections which exhibited no visible cracking or minimal map cracking, as shown in Figure 2.1. The moderate damage level included sections which exhibited moderate map cracking and/or longitudinal cracks, as shown in Figure 2.2. Severe damage included sections which exhibited severe map cracking, longitudinal cracks (greater than 2 mm), crushing at the joints, and/or alkali-silica gel exudation and precipitation near cracks. A typical section with severe damage is shown in Figure 2.3.

Figure 2.1. A median barrier section which exhibits minimal damage, (e.g. 3no visible map cracking). Picture used with permission from Richard Deschenes.

The visual damage survey results were compiled and utilized in the development of a plot of damage with respect to interstate log mile. The length, in miles, of median barrier which exhibits each damage level was also reported to evaluate the extent of sections which require rehabilitated with each treatment method, and the feasibility of each treatment. Due to

variability of damage along the median barrier, a system of surface treatments was evaluated. A surface treatment which works effectively on the sections with minimal damage, may not work for the sections with severe damage.

Figure 2.2. A typical median barrier section which exhibits moderate damage, (e.g. moderate visible map cracking, and a longitudinal crack along the full length of the section). Picture used with permission from Richard Deschenes.

In addition, a treatment which is effective on sections with severe damage is impractical for use along the entire 4.4 mile median barrier. Therefore, sections from all three damage level were selected for the evaluation of several surface treatment regimes.

Figure 2.3. A typical median barrier section which exhibits severe damage, (e.g. severe map cracking, longitudinal cracks, crushing at the joints, and visible alkali-silica gel exudation). Picture used with permission from Richard Deschenes.

2.1.3 Review of Construction Documents

Construction documentation was an additional source of information required to determine the cause of deterioration within the median barrier. The documentation included information on the sources of materials used in the concrete median barrier, such as aggregates and cementitious materials. The concrete mixture proportions were the same throughout the length of the median barrier, however, the mineralogy of the cement changed with each batch. Therefore, information regarding the cement source and mineralogy was required to understand the variability of damage levels along the median barrier. The aggregate sources used for the concrete mixture were also important in determining the source of reactive siliceous minerals within the concrete. The concrete mixture design included information on the amount of each aggregate and cementitious material, which was useful for laboratory evaluation.

Some of the construction documentation was destroyed before the research program began. However, limited information on the aggregate sources and cement chemistry was available, and the information could not connect the cement chemistry for each batch of concrete to the corresponding section of the median barrier. However, the information was used to understand the source of ASR and variability of damage along the median barrier. There was limited information on the concrete mixture design, and the results from petrographic analysis were used to determine the concrete properties.

2.2 Laboratory Research

The laboratory investigation of the aggregates used within the concrete median barrier was invaluable in the determination of sources of reactive aggregate and the source of ASR. A review of relevant literature concluded that two common test methods were available for the

evaluation of potentially alkali-silica reactive aggregates. The first test method was the AMBT, which was used to rapidly screen aggregates for potential expansion due to ASR, and the results were verified by additional testing. The second test method, the concrete prism test (CPT), was used to confirm the potential for alkali-silica reactivity of an aggregate. The combination of AMBT and CPT tests was used to determine which aggregates contribute reactive silica to the concrete and have the potential to develop ASR. The results were also compared to the petrographic examination to clarify any contradictions.

Fly ash was used in the median barrier concrete, which changes the mechanism by which ASR develops. Additional testing was required to determine if the fly ash was a factor in the development of ASR. A modified AMBT was utilized to evaluate aggregates with a combination of cementitious materials.

2.2.1 Material Sources

The construction documentation and the petrographic examination results were reviewed to locate original materials used within the median barrier. Fine aggregate from Van Buren, Arkansas is commonly used for concrete throughout the region, and was readily available for evaluation. The sand used for laboratory evaluation was dredged from the Arkansas River in 2012 and was representative of the sand used in the concrete median barrier in 1998. The limestone coarse aggregate quarry in West Fork Arkansas was no longer in operation. However, some representative material was stockpiled at the quarry and was available for laboratory evaluation. The original cement used in the median barrier was not available for evaluation. However, accelerated laboratory test methods are not affected by cement chemistry. Therefore, the original cement is not required for laboratory evaluation. The cement used in the median

barrier concrete was manufactured in Pryor Oklahoma between 1998 and 1999. Records of cement chemistry were available and utilized to determine the cause of ASR within the median barrier concrete. The fly ash used within the median barrier concrete was Class C fly ash produced at the OG&E coal power plant in Muskogee, Oklahoma. Fly ash chemistry records for 1998 to 1999 were available for the median barrier concrete.

2.2.2 AMBT (ASTM C1260)

The AMBT has a short test duration (16 days) which allows for rapid evaluation of aggregates for potential alkali-silica reactivity. The test method was conducted in accordance with ASTM C1260 Standard Test Method for Potential Alkali Reactivity of Aggregates (Mortar-Bar Method). The aggregate was first sieved to the standard gradation and then a standard batch of mortar was mixed. When evaluating coarse aggregates, the aggregate was first crushed and then sieved to match the gradation. The aggregate gradation and batch weights to produce three mortar bars are summarized below in Table 2.1.

Table 2.1. ASTM C1260 standard gradation and batch weights.

	No. 8	No. 16	No. 30	No. 50	No. 100	Cement	Water
Fraction	10	25	25	25	15	--	0.47
Mass (g)	99	247.5	247.5	247.5	148.5	440	206.8

The standard batch produced enough mortar for three mortar-bars with standard dimensions of 25 x 25 x 285 mm (1 x 1 x 11.25 in). The mortar bars were cured for 24 hours in an environmental chamber with ambient temperature of 23 ± 2 degree Celsius and 95 percent relative humidity. The mortar-bar molds are displayed in Figure 2.4 (left), and typical cured mortar-bars are displayed in Figure 2.4 (right).

Figure 2.4. Mortar-Bar mold with gage studs (left) and mortar-bar mold with three mortar-bars (right). Picture used with permission from Richard Deschenes.

The mortar bars were removed from the molds after 24 hours of curing. The mortar-bars were then placed in 80 degrees Celsius water for 24 hours. A typical set of cured mortar bars are displayed in Figure 2.5 (left), and a typical set of mortar-bars in the storage containers are displayed in Figure 2.5 (right).

Figure 2.5. Mortar-bars (left) and mortar-bar in storage container (right). Picture used with permission from Richard Deschenes.

The initial length-change of each mortar-bar was measured after 24 hours in the water bath. The mortar-bar temperature equilibrates when exposed to air, and the length-change for each mortar-bar is measured within 15 ± 5 seconds of being removed from the container to reduce thermal shrinkage. The three mortar-bars were measured, and then moved to a container of 1N sodium

hydroxide (NaOH) solution which was stored at 80 degrees Celsius. The mortar-bars were stored in the sodium hydroxide (NaOH) solution for 14 days. Length-change measurements were ascertained a minimum of three times during the 14 day storage period.

The sodium hydroxide (NaOH) solution was produced by dissolving 40 grams of sodium hydroxide (NaOH) pellets in 900 ml of water. After the sodium hydroxide (NaOH) pellets dissolved, the solution was diluted to obtain 1.0 L of solution. The required volume of solution within the storage container is four times the volume of the mortar-bars. The sealed containers were stored in a water bath at 80 degrees Celsius for the duration of the test.

The final length-change was determined after 14 days of storage. The interim measurements were ascertained at 4 and 7 days of storage. The length-change was measured with a comparator and digital gage with a precision of 0.001 percent of the effective gage length. The length-change of the three mortar-bars was averaged, and reported to the nearest 0.01 percent. The final length-change was then compared to the expansion limits. Expansions less than 0.10 percent at 16 days indicate innocuous aggregates. Expansion between 0.1 and 0.2 percent at 16 days require additional information to establish aggregate reactivity. In addition, the specification allows a test duration of 28 days for samples with 14 day expansions between 0.1 and 0.2 percent. Mortar-bars with 14 or 28 day expansion greater than 0.20 percent indicate potentially deleteriously expansive aggregates.

The results of each AMBT was compiled and plotted with time (days) on the abscissa and length-change (percent) on the ordinate axis. The AMBT storage conditions necessary to accelerate ASR and prevent alkali-leaching are harsh and often produce excessive expansion in

aggregates with proven field performance. Therefore, the AMBT results were compared to CPT results to confirm the aggregate classification.

2.2.3 CPT (ASTM C1293)

The CPT is the most reliable accelerated test method available for evaluating aggregates for alkali-silica reactivity. The test duration, one year or longer, is somewhat prohibitive; however, the test is highly recommended for use in laboratory research. The advantages of the CPT are numerous, and include the ability to test concrete mixtures as well as coarse aggregates without first crushing the aggregates. The test also allows for the evaluation of combinations of cementitious materials for the prevention of ASR.

The CPT was conducted in accordance with ASTM C1293 Standard Test Method for Determination of Length Change of Concrete Due to Alkali-Silica Reaction. The requirements for a CPT standard concrete mixture were provided in the specification. The coarse aggregate was sieved to the standard gradation as specified in ASTM C1293. The concrete mixture required a coarse aggregate oven-dry-rodded unit volume of 0.70 ± 0.2 percent. The water to cementitious material ratio (w/cm) was specified between 0.42 and 0.45 (by mass). The volume fraction of sand was selected to produce a unit volume of concrete. The cement content was specified as 420 kg/m^3 (708 lb/yd^3), and the cement alkali content was limited to 0.90 ± 0.1 percent Na_2O_e.The alkali content was increased to 1.25 percent Na_2O_e by the addition of sodium hydroxide (NaOH) to the mixture water before batching. The required sodium hydroxide was determined from the cement and cement alkali content. Unfortunately, the only available cement at the time of testing was 0.53 percent Na_2O_e by mass, and additional sodium hydroxide (NaOH)

was required to achieve the required alkali level. The mixture proportions used for the CPT are summarized below in Table 2.2.

After the concrete mixture was batched, slump, unit weight, and air content tests were performed in accordance with ASTM C143, and ASTM C138, respectively. Concrete was then placed into the prism molds in two lifts, with rodding and tamping after each lift to ensure sufficient compaction. The prisms are 75 x 75 x 285 mm (3 x 3 x 11.25 in) and are displayed below in Figure 2.6. A total of three prisms were required for each concrete mixture evaluated. After trowelling the top of the prisms, the molds were placed and cured in the environmental chamber for 24 hours.

Table 2.2. ASTM C1293 mixture design specifications and typical batch weights.

	Notes	kg/m^3 (lb/yd^3)
Coarse	0.70 ± 0.05 D.R.U.W.	1110 (1871)
1/2	33%	370 (624)
3/8	33%	370 (624)
No. 4	33%	370 (624)
Sand	F.M ~ 2.7	629 (1060)
Cement	~ 0.90% Na_2O_e	420 (708)
Water	w/cm ~ 0.45	189 (319)
NaOH	1.25% Na_2O_e	1.90 (3.20)

After curing, the prisms were removed from the molds and the initial length-change was measured using a length-change comparator with a digital gage. The prisms were then placed in the storage containers and placed in a water bath at 38 degrees Celsius. The duration of length-change monitoring was one year, with interim readings taken at 7, 28, 56 days, 3, 6, 9, and 12 months. The storage containers were removed from the water bath 16 ± 4 hours before length-change readings to allow the temperature of the prisms to equilibrate to room temperature. The storage containers must also maintain a high relative humidity (ASTM, 2012). The containers

used for storage had dimensions of 225 x 300 x 112 mm (9 x 12 x 4.5 in.) with a water tight cover. The prisms were elevated 25 mm (1 inch) from the bottom of the container with small blocks of wood, and then 12.5 mm (1/2 inch) of water was placed in the bottom of the container. The containers were sealed and placed in a water bath to maintain a temperature of 38 degrees Celsius.

Figure 2.6. Typical CPT prism molds (left), and storage containers (right). Picture used with permission from Richard Deschenes.

No wicking material was used along the inside edges of the containers. Therefore, there was some concern that water precipitated on the surface of the prisms and transported alkalis from the surface of the prism into the water at the bottom of the container. Additionally, some of the containers leaked during storage and allowed water within the container to make contact with the bottom of the prisms. Therefore, alkalis likely leached out of the prisms during storage. Alkali leaching may have reduced the validity of the results from the concrete prism tests. This is discussed in greater detail in Chapter 3. The ASTM C1293 specification recommends 19 to 21 L (5 gallon) pails with sealed covers for storage of concrete prisms. The specification also recommends polypropylene fabric used along the inside of the containers to wick moisture and

prevent alkalis from being leached out of the prisms. However, the recommended pails require a large water bath or environmental chamber for storage of several samples. Due to limited availability of space, smaller containers were selected to increase the number of samples evaluated simultaneously.

After one year of monitoring, results from the three prisms were averaged to produce a single plot. The data were plotted with time (days) on the abscissa and length-change (percent) on the ordinate axis. A one-year expansion greater than 0.04 percent indicates a concrete mixture with potentially deleterious expansion. The CPT provides the most reliable accelerated method of evaluating aggregates for alkali-silica reactivity. However, precautions are necessary to prevent or reduce alkali-leaching. The effects of alkali-leaching were not apparent until 6 to 9 months of monitoring.

Preventative measures against ASR are also evaluated with the CPT method. Preventative measures include supplementary cementitious materials or lithium nitrate. Due to the effects of SCMs on the mechanisms of ASR, the test duration is extended to two years. Time limitations prevented the evaluation of SCMs with this test method during the current research project.

2.2.4 AMBT with SCMs (ASTM C1567)

The AMBT method accelerates the development of ASR by storing the mortar-bars at 80 degrees Celsius. The sodium hydroxide solution prevents alkalis from leaching from the mortar bars during storage. The storage environment accelerates the development of ASR and provides results in 16 days. Due to the harsh storage conditions the test method can produce expansion in cement-aggregate combinations which have a good field performance history. However, when evaluating preventative measures against ASR the test method can produce conservative

estimates on the required level of prevention. The AMBT method allows for the evaluation of cement-aggregate mixtures with a partial replacement of cement with SCMs. The test was conducted in accordance with ASTM C1567 Standard Test Method for Determining the Potential Alkali-Silica Reactivity of Combinations of Cementitious Materials and Aggregate (Accelerated Mortar-Bar Method). The test method is identical to the AMBT with the exception of the cementitious materials. Fly ash, silica fume, slag cement, and metakaolin are evaluated at various replacement rates to determine the minimum safe replacement rate which will prevent ASR expansion. A 16 day expansion less than 0.10 percent signifies a safe replacement rate. Some SCMs, such as fly ash, delay alkali-silica reactivity and the AMBT duration is extended to 28 days to allow for any delayed reactions.

Fine aggregate from the Arkansas River was evaluated in combination with class C fly ash. The fly ash was sourced from the same location as the fly ash used within the median barrier, and had a similar chemical composition. Tests were conducted at several fly ash replacement rates ranging from 10 to 40 percent replacement by weight of cement. The safe replacement rate was determined through an evaluation of replacement rates below and above the safe range. The replacement rate which provided 30 day expansion below 0.10 percent was then determined. The test duration was increased to 28 days to account for any delayed reactions due to the fly ash.

2.3 Field Monitoring

The next phase of research involved monitoring expansion and relative humidity within several sections of the median barrier followed by surface treatment. The sections were monitored for one year, with periodic interim measurements. Each of the surface treatments was evaluated on

median barrier sections of each damage level, and compared to a control section at each damage level. The median barrier was instrumented with monitoring equipment on January 31, 2013 and then treated on March 12, 2013. The final measurements were performed on January 14, 2014.

2.3.1 Instrumentation

The first stage of field monitoring required instrumenting the median barrier for length-change and internal relative humidity monitoring. A total of 15 sections were selected for instrumentation. Five sections were selected from each damage level. Length-change was measured with a detachable mechanical strain gage (DEMEC) which measures the distance between two gage studs which were affixed to the median barrier. The points were affixed to the median barrier by drilling 9.5 mm (3/8 inch) diameter holes, 75 mm (3 inch) into the vertical face of the median barrier. Four holes were drilled at the corners of a 500 x 500 mm (20 inch) square grid. A typical length-change grid is shown in Figure 2.7.

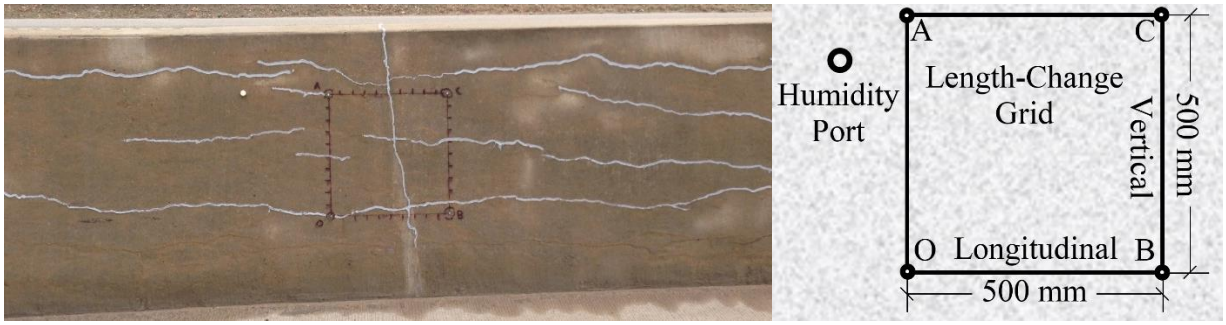

Figure 2.7. Typical length-change grid (left) and dimensions (right). Picture used with permission from Richard Deschenes.

Stainless steel gage studs were machined with dimensions of 8 mm (5/16 inch) diameter by 75 mm long. A small point (1 mm by 3 mm deep) was drilled into the end of the gage stud. The points on the DEMEC gage were inserted into the points in the gage studs when measuring the

distance between two gage studs. A gage stud which was affixed to the median barrier is shown in Figure 2.8 (left) and a humidity port is shown in Figure 2.8 (right).

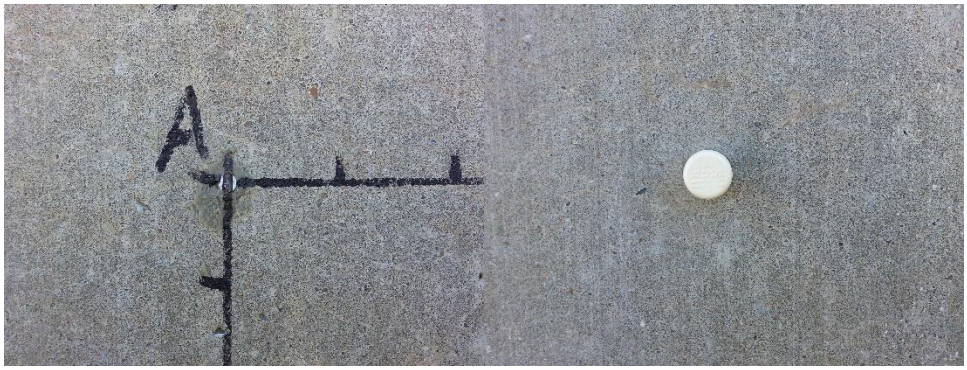

Figure 2.8. Typical gage stud (left) and humidity port with cap (right). Pictures used with permission from Richard Deschenes.

The length-change was measured along the four sides of the grid, and then the DEMEC gage was reversed and the four sides measured again. The length-change for each side of the grid was then determined from the average of the two measurements. The DEMEC gage reports the length-change with a precision of ±0.00005 percent. The length-change was subtracted from the previous reading to determine the difference. The difference was then divided by the gage length (500 mm) and multiplied by 100 percent. The final value was reported as percent strain with a precision of 0.0001 percent. The DEMEC gage is displayed in Figure 2.9 (right) while measuring length-change in the longitudinal direction.

A hole was also drilled to the left of each length-change grid for inserting the internal relative humidity probe. The hole was 16 mm (5/8 inch) diameter and 125 mm (5 inches) deep. The port was capped with a 12.5 mm inside diameter CPVC pipe and tight-fitting plastic cap. The cap was easily removed for measurements and was intended to prevent moisture from entering or exiting the port. During measurements, the humidity probe was inserted into the port and

allowed to equilibrate with the concrete for 30 minutes. The probe was left in the port until there was less than ±1 percent change in internal relative humidity over a five minute period, but no less than 15 minutes total time. Ideally, one hour was required to allow the conditions within the port to reach equilibrium with the concrete. However, time was limited and only 30 minutes was available to measure each median barrier section. In addition, because the ports were sealed before measurements were taken; the ambient conditions within the port were already in equilibrium with the concrete. Once the humidity probe was inserted into the port and the temperature of the probe reached equilibrium with the concrete no additional time was required for equilibrium to occur. After the probe temperature reached equilibrium with the concrete, subsequent sections took less time because no additional time for equilibrium conditions was required. The portable humidity indicator and humidity probe are shown in Figure 2.9 (center) and Figure 2.9 (right), respectively.

Figure 2.9. DEMEC gage during length-change measurement (left), portable humidity indicator (center), and humidity probe inserted into a humidity port (right). Pictures used with permission from Richard Deschenes.

2.3.2 Treatment

Two months after instrumenting the median barrier for monitoring length-change and internal relative humidity the selected sections were treated with a surface treatment. The goal of surface

treatment was to reduce the internal relative humidity within the concrete to a level below 80 percent. Several commercial surface treatments were available for protecting concrete from external moisture. Due to the variability in the level of damage throughout the length of the median barrier, three surface treatments were selected based on information collected during the literature review. The first treatment method evaluated was silane, which was used successfully by Berube et al. (2002b) to treat concrete median barriers with ASR damage. However, silane has proven less effective in extensively cracked sections. Therefore, an elastomeric breathable vapor barrier was also examined to evaluate moisture protection for sections with wider cracks. The third treatment, boiled linseed oil, was selected because of its accessibility and proven history as a method of protecting bridge-decks from moisture. The application rate and material cost for each treatment is summarized in Table 2.3. The silane and linseed oil were applied with hand sprayers while the elastomeric paint was applied with paint rollers. An additional consideration was the much more labor-intensive application of elastomeric paint which required paint rollers.

Table 2.3. Material cost and application rate for surface treatments.

Treatment	Silane	Elastomeric Paint	Linseed Oil
Brand	Enviroseal 40	Sikagard 550w	Euclid Linseed Oil
Cost, 19L (5 gal)	$217	$248	$174
Application Rate, m^2/L (ft2/gal)	3.7 (150)	2.5 (100)	7.4 (300)
Cost, $/$m^2$ ($/ft2)	$3.12 ($0.29)	$5.34 ($0.50)	$1.25 ($0.12)

There were five sections of median barrier selected for treatment from each of the three damage levels. The first section was left untreated as a control, the second section was sprayed with a single application of silane, the third section was sprayed with a single application of linseed oil, the fourth section was painted with elastomeric paint, and the fifth section was sprayed with a

single application of silane and then an additional application of silane six months later. A typical application of surface treatments is shown in Figure 2.10 (left). To ensure the correct application rate, the required amount of each respective treatment for a single section was measured and then applied to the section. The sections were allowed to dry for 24 hours, and then initial length-change and internal relative humidity were measured. Several of the moderately and severely damaged sections exhibited wide cracks (> 2 mm) which were sealed with silicon sealant to prevent excess moisture from entering the concrete. The silicon crack sealant is shown as applied in Figure 2.10 (right).

Figure 2.10. Application of surface treatment (left) and crack sealant (right). Pictures used with permission from Richard Deschenes.

2.3.3 Monitoring

Periodic measurements of length-change and internal relative humidity were performed on the fifteen median barrier sections. Measurements were performed monthly for the first six months and then at nine months and one year. Measurements included vertical and longitudinal length-change for each median barrier section. The measurements were performed as described above, and each length-change axis represents the average of four measurements. The DEMEC gage reference points were first inserted into gage studs ‘A’ and ‘O’ (Figure 2.7) of the length-change

grid and the length-change was reported to ±0.00005. This process was then repeated for the three remaining sides of the grid. The DEMEC gage was then reversed and a second measurement taken for each side of the grid. Therefore, the length-change was measured twice on each side of the length-change grid. The two length-change measurements for each side of the grid were then averaged to minimize error. After the average percent strain for each side of the grid was determined, the two vertical sides were averaged to produce a single value which represents the percent strain in the vertical axis of the median barrier section. This process was repeated for the two longitudinal sides of the length-change grid to produce an average percent strain in the longitudinal direction. However, the longitudinal strain results were not useful because expansion was prevented by the internal and external restraint on the median barrier sections. The raw longitudinal strain data is provided in Appendix A1.4. Simultaneous to length-change measurements, the internal relative humidity and temperature were measured using a Vaisala SHM40 portable humidity indicator and probe. The probe was inserted into the port and allowed to equilibrate with the conditions within the concrete. A minimum of fifteen minutes was allowed for equilibrium to occur, and the reading was reported after the internal relative humidity changed less than ±1 percent within five minutes. This process was repeated for all fifteen median barrier sections.

2.3.4 Data Reduction

After measuring internal relative humidity and strain, the data was normalized and plotted for each section. The sections of each damage level were plotted in the same graph to allow for comparison of each treatment method. The strain rate and differential strain for each section was determined to describe the efficacy of each treatment in reducing strain as compared to the control.

2.3.4.1 Temperature Normalized Data

The first step in reducing the DEMEC measurements into strain was to apply a unit multiplier of 0.80 to the raw measurement. The DEMEC gage utilizes a lever between the point which is inserted into the gage stud and the point which actuates the digital strain gage. The lever has a ratio of 0.8:1.0 and an increment of 1.0 at the gage stud represents an increment of 0.8 at the strain gage. After applying the multiplier, the percent strain was determined by first subtracting the strain at the current date from the initial strain at day-0. The difference was then divided by the DEMEC gage length and then multiplied by 100 percent. The actual gage length was 500 mm ± the day-0 reading, to account for the initial variation between the DEMEC gage and the measurement grid. The process for percent strain is shown below in Equation 2.1.

$$\text{Strain } (\%) = \frac{\Delta_i - \Delta_0}{L_g + \Delta_0} \times 100\% \qquad \textbf{Equation 2.1}$$

$$\Delta_i = 0.8 \times \text{DEMEC}_i$$
$$\Delta_0 = 0.8 \times \text{DEMEC}_0$$
$$L_g = 500 \text{ mm} = 19.685 \text{ in.}$$

The strain data was then normalized for an ambient temperature of 24 degrees Celsius to remove thermal strains. A coefficient of thermal expansion (CTE) of 10×10^{-6} per degree Celsius was selected for the concrete. Although the actual CTE was not measured for the median barrier, the CTE for concrete typically falls between 8×10^{-6} and 12×10^{-6} per degree Celsius. The temperature normalization is shown in Equation 2.2.

$$\text{Strain } (\%) = \frac{(\Delta_i + \Delta_{Ti}) - (\Delta_0 + \Delta_{T0})}{L_g + (\Delta_0 + \Delta_{T0})} \times 100\% \qquad \textbf{Equation 2.2}$$

$$\Delta_{Ti} = \text{CTE} \times L_g \times (T_{24} - T_i)$$
$$\Delta_{T0} = \text{CTE} \times L_g \times (T_{24} - T_0)$$

The temperature normalized data was then plotted with strain (percent) on the ordinate, and time (days) on the abscissa. The strain rate was determined from the best-fit line of the data, with the intercept set to the origin. The R^2 value for the best fit line was also determined to show the variation between the data and the best-fit line.

2.3.4.2 Temperature Normalized Internal Relative Humidity Data

An attempt was made to normalize the relative humidity data to a temperature of 24 degrees Celsius. However, the temperature normalization process lead to the realization that the system for measuring internal relative humidity was flawed. As the temperature increases within a closed system, in which there is a constant mass of air and water, the relative humidity should decrease. However, the ports used for inserting the humidity probe into the median barrier did not form a closed system. Water entered the port from outside the concrete and allowed the relative humidity within the port to increase as temperature increased. It was not possible to normalize internal relative humidity to realistic values which represent the relative humidity within the concrete. Therefore, the internal relative humidity data was not normalized and does not represent the relative humidity within the concrete at 21 to 24 degrees Celcius. However, the relative humidity data, especially for sections of minimal damage, provided a comparison between the treated and control sections.

3 Results

As stated earlier, the research program was conducted in three phases, which included a preliminary investigation, laboratory research, and field monitoring. The laboratory research and field investigation phases were conducted simultaneously. However, the preliminary investigation was invaluable in the development of the plan of research. The results of the three research phases are presented below.

3.1 Preliminary Investigation

3.1.1 Petrographic Analysis

A petrographic examination of concrete core samples extracted from the median barrier was performed in 2012 by Construction Technology Laboratories Group (CTLGroup). The petrographic examination concluded that the concrete contained 1.0 in crushed limestone coarse aggregates and natural sand fine aggregates. The concrete was not air-entrained and contained 3 to 4 percent air in randomly distributed voids. The concrete contained an estimated 10 to 15 percent fly ash by weight.

Deposits of alkali-silica gel were found associated with chalcedony fine aggregate particles. The chalcedony fine aggregate particles were primarily located within the coarse portion of the fine aggregates. The chalcedony particles had alkali-silica reaction rims, and gel deposits had filled some air voids. Micro-cracking was discovered throughout the depth of the concrete, with cracks originating from alkali-silica gel deposits. Freezing and thawing deterioration was noted as a secondary form of distress, which exacerbated the deterioration. Micro-cracking due to ASR allowed excess water to enter the concrete and freeze, which then increased the extent of deterioration.

3.1.2 Visual Inspection

A visual inspection of the median barrier was conducted in January 2013 to determine the extent of deterioration throughout the length of the median barrier. Sections of median barrier were divided into one of three categories based on the level of visible distress. The classification was logged with respect to mile marker of interstate and then plotted in Google Earth to visualize the extent of distressed sections. The plot of damage along the median barrier is shown in Figure 3.1. The length of median barrier which exhibited distress of each damage designation is summarized in Table 3.1. The color corresponding to each damage designation is the same as shown in Figure 3.1. Five median barrier sections of each damage designation were selected for monitoring and treatment.

Table 3.1. Length of median barrier sections which correspond to each damage designation.

Damaged Sections (Miles)			
Minimal	Moderate	Severe	Total
2.3	1.40	0.7	4.40

Figure 3.1. Median barrier damage level along Interstate 49. Figure produced in Google Earth.

3.1.3 Construction Documents

Limited documentation from the construction of the median barrier was available at the start of the research program. However, information was available on the sources of aggregate, cement, and fly ash. Cement and fly ash chemistry were recovered from the original manufacturers. As discussed earlier, the fine aggregate was obtained from the Arkansas River in Van Buren, AR. The coarse aggregate was acquired from the limestone quarry in West Fork, AR. The cement was obtained from Pryor, Oklahoma and the Class C fly ash from Muskogee, Oklahoma. The cement alkali levels in percent Na_2O_e, for the cement used in the median barrier are summarized in Figure 3.2.

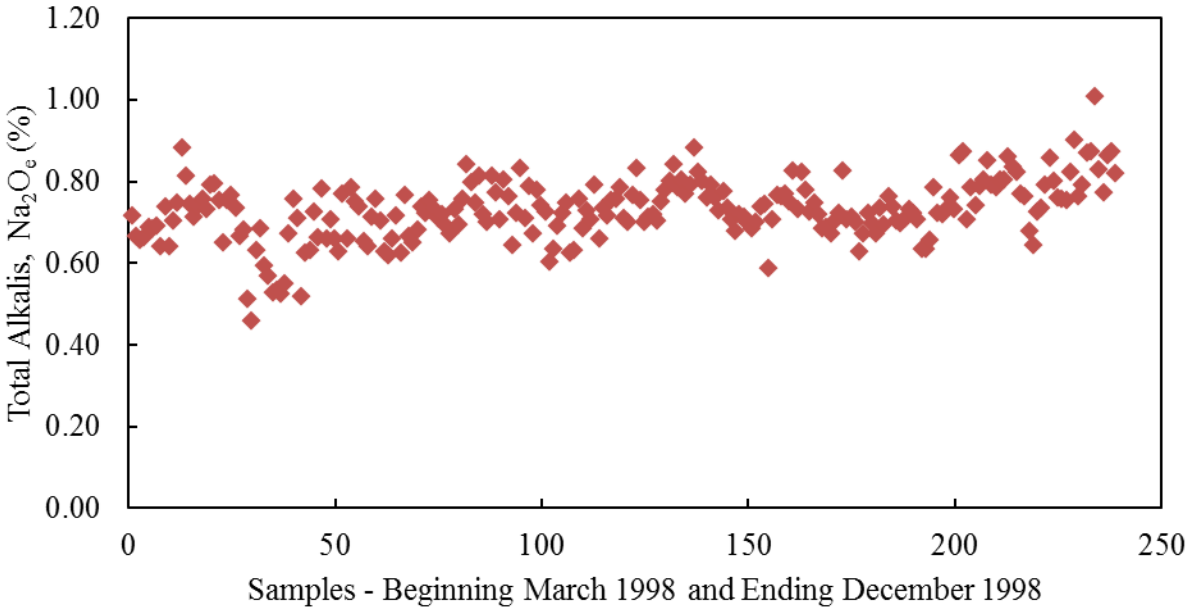

Figure 3.2. Cement alkali content (Na_2O_e) with respect to time.

The Class C fly ash contained roughly 25 percent lime (CaO) by weight, and available alkalis of 1.31 percent Na_2O_e. The cement alkali level varied, which explains the variation in damage along the median barrier. The actual alkalis in each section of median barrier were unknown.

However, the sections of moderate or severe damage likely contained higher alkali cement than the sections of minimal damage.

3.2 Laboratory Research

The laboratory research phase included ASTM C1260 and ASTM C1293 tests, which are common standard test methods for evaluating aggregates for deleterious expansion due to ASR. Additional tests were conducted, in accordance with ASTM C1567, to evaluate fly ash as a preventative measure. The aggregates tested included those from the original sources used during the median barrier construction, as well as several samples of regionally available aggregates which are used in concrete.

3.2.1 Material Sources

Original samples of the aggregates and cementitious material used during the construction of the median barrier were no longer available. Therefore, new samples of Van Buren river sand were collected from the original source. In addition, a stockpile of West Fork limestone was available for testing. The cement used during laboratory tests contained 0.53 percent Na_2O_e, as compared to the median barrier cement which contained between 0.46 and 1.0 percent Na_2O_e. Fortunately, the cement alkali level does not affect the outcome of the AMBT. In addition, the cement alkalis were increased to 1.25 percent Na_2O_e for the CPT concrete mixtures.

Several additional aggregate sources from the region were evaluated during laboratory testing to locate any additional potential sources of ASR. However, these tests were not vital to determining the cause of ASR, or developing mitigation methods for ASR in the median barrier.

3.2.2 AMBT (ASTM C1260)

The AMBT was conducted in accordance with ASTM C1260. The aggregates evaluated were first crushed and then sieved to meet the specification. Three mortar bars were produced following the specified mortar mixture. The mortar bars were cured and stored in accordance with ASTM C1260. The mortar bars were periodically measured throughout the 16 day test duration and the strain recorded. For each aggregate evaluated, the strain was determined from the average strain of six mortar bars. The AMBT results are summarized in Figure 3.3 and discussed below. The strain is shown in percent and the time in days. Each aggregate tested is labeled with the city of origin and type of aggregate. The individual batch information is summarized in Appendix A1.1.

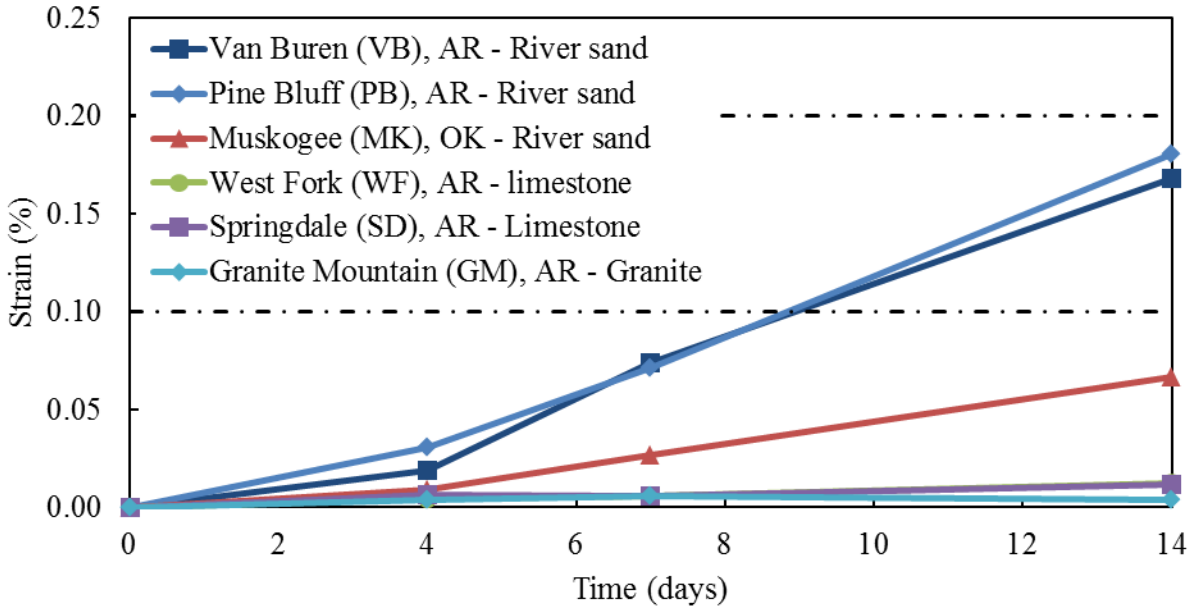

Figure 3.3. Strain (%) with respect to time (days) results for ASTM C1260 tests.

Van Buren (VB) – Mortar bars which contained river sand from Van Buren, Arkansas exhibited a 14 day expansion of 0.17 percent. The aggregate sample was therefore classified as

'potentially deleteriously reactive.' Due to harsh conditions during storage of mortar bars, additional tests are recommended for aggregates which produce a 14 day strain between 0.10 and 0.20 percent. Therefore, ASTM C1293 tests were performed on samples of this aggregate. In addition, a petrographic analysis of concrete from the median barrier discovered that river sand from Van Buren Arkansas was the source of reactive silica in the development of ASR.

Pine Bluff (PB) - Mortar bars which contained river sand from Pine Bluff, Arkansas developed very similar strain to that of mortar bars which contained Van Buren river sand. The 14 day strain for mortar bars which contained Pine Bluff river sand was 0.18 percent, which also results in classification as 'potentially deleteriously reactive.' The ASTM C1293 test was performed on this aggregate to verify the results. A Petrographic analysis of concrete which contained river sand from Pine Bluff Arkansas also concluded that the aggregate contained silica which developed ASR.

Muskogee (MK) –The 14 day expansion for mortar bars which contained a sample of river sand from Muskogee, Oklahoma was 0.07 percent. The aggregate was classified as 'inert.' There were no reported cases of ASR in concrete which contains this aggregate known to this author.

West Fork (WF) - Mortar bars which contained a crushed sample of limestone coarse aggregate from West Fork, Arkansas developed a 14 day expansion of 0.01 percent, and the aggregate was classified as 'inert.' The limestone aggregate sample was crushed to match the specified gradation in ASTM C1260. Aggregate from the same source were used in concrete which developed ASR. However, it was discovered through petrographic analysis that the aggregate did not contribute to the development of ASR.

Springdale (SD) - Mortar bars which contained limestone coarse aggregate from Springdale, Arkansas exhibited similar strain to that of West Fork limestone. The 14 day expansion was 0.01 percent, and the aggregate was classified as 'inert.' The fine aggregate limestone sample was produced through sieving the fine material from a sample of ¾ inch nominal aggregate. No cases of ASR in concrete which contained this aggregate were known to this author.

Granite Mountain (GM) - The 14 day expansion for mortar bars which contained granite from Granite Mountain, Arkansas was 0.004 percent. The sample was also produced through sieving a larger sample of ¾ inch nominal aggregate. Again, no cases of ASR in concrete which contains Granite Mountain granite were known to this author.

3.2.3 CPT (ASTM C1293)

The concrete prism tests were conducted in accordance with ASTM C1293. The coarse aggregates selected for evaluation were first sieved to meet the specification. A non-reactive fine aggregate was tested under AMBT conditions and then used when evaluating coarse aggregates. When fine aggregates were evaluated, a non-reactive coarse aggregate was first evaluated under AMBT conditions and then sieved to match ASTM C1293 specifications before use in the CPT. Three concrete prisms were produced using the specified concrete mixture. The prisms were cured and stored in accordance with ASTM C1293. The prisms were measured at the prescribed times and the strain recorded. Each strain measurement was developed from the average strain of six prisms. The CPT results are summarized in Figure 3.4 and discussed below. The strain is shown in percent and the time in days. Each aggregate tested is labeled with the city of origin and type of aggregate. Mixture designs, slump, unit weight, air content, and batch temperatures are summarized in Appendix A1.2.

Van Buren (VB) - The one year strain for prisms which contain river sand from Van Buren, Arkansas was 0.028 percent. As specified in ASTM C1293, a one year strain greater than 0.04 percent indicates 'deleteriously expansive aggregates.' The aggregate was therefore classified as 'inert', which contradicts the results of ASTM C1260 test. However, petrographic examination of concrete from the median barrier determined that river sand from Van Buren, Arkansas was the source of ASR. As stated earlier, the CPT is an accurate test method, which rarely provides invalid results. The strain results of the tests conducted on Van Buren river sand was lower than expected due to alkali leaching during storage of the prisms. Due to limited space, the prisms were not stored in the method recommended by ASTM C1293. Therefore, alkalis were leached from the prisms and expansion was reduced.

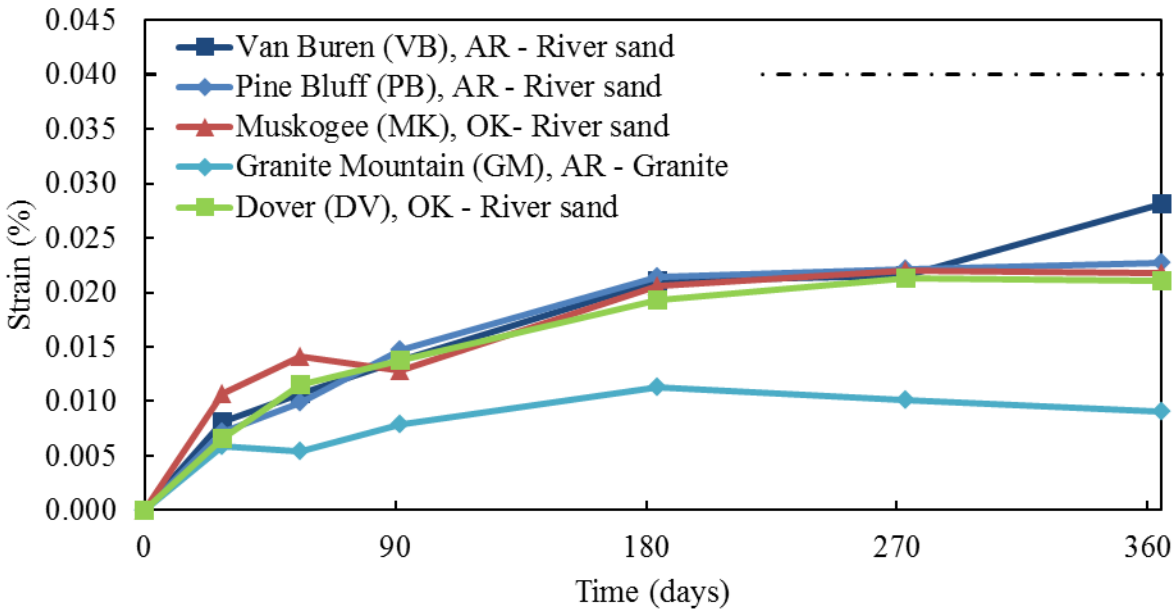

Figure 3.4. Strain (%) with respect to time (days) results for ASTM C1293 tests.

Pine Bluff (PB) – Prisms which contained river sand from Pine Bluff, Arkansas developed a one year expansion of 0.023 percent. The one year expansion was lower than the failure criterion

proposed in ASTM C1293. The aggregate was classified as 'inert', which again contradicted the results of AMBT and a petrographic examination of concrete which contained aggregate from the same source.

Muskogee (MK) – Concrete prisms which contained river sand from Muskogee, Oklahoma exhibited a one year expansion of 0.022 percent. The aggregate was therefore classified as 'inert.' However, this result agrees with the AMBT, and no known cases of ASR have been reported in concrete which contains river sand from Muskogee, Oklahoma.

Granite Mountain (GM) - A sample of granite coarse aggregate from Granite Mountain, Arkansas was subjected to the CPT, and prisms which contained the aggregate developed a one year expansion of 0.009 percent. The aggregate was therefore classified, in agreement with AMBT results, as 'inert.'

Dover (DV) – Prisms which contained river sand from Dover, Oklahoma developed a one year expansion of 0.021 percent. The aggregate was classified as 'inert,' and no AMBT results are available for this aggregate sample. However, no instances of ASR in concrete which contain this aggregate are known to this author.

3.2.4 AMBT with SCMs (ASTM C1567)

A modified AMBT was utilized to evaluate SCMs as a preventative measure against ASR. The test was conducted in accordance with ASTM C1567, which is similar to ASTM C1260 with the exception of SCMs used in the mixture. In addition, the test duration is often extended to 28 days to account for delayed hydration caused by some SCMs. The aggregates evaluated were first crushed and then sieved to meet the specification. Three mortar bars were produced using the specified mortar mixture with a selected portion of the cement being replaced with fly ash.

The mortar bars were cured and stored in accordance with ASTM C1567. The mortar bars were periodically measured and the strain recorded. Each strain result was developed from the average strain of three mortar bars. The results are summarized in Figure 3.5 and discussed below. The strain is shown in percent and the time in days. Each aggregate tested is labeled with the city of origin and type of aggregate.

Van Buren (VB) –As apparent in Figure 3.3, mortar bars which contained river sand from Van Buren, Arkansas exhibited a large strain rate at the end of the 16 day test duration. As recommended in ASTM C1260 Appendix X1.1.3, an additional test with an extended duration of 28 days was performed on a sample of river sand from Van Buren (ASTM 2008a). As shown in Figure 3.5, the 28 day expansion for mortar bars which contained river sand from Van Buren was 0.25 percent. Therefore, the aggregate is classified as 'deleteriously reactive' in accordance with ASTM C1260 Appendix X1.1.2 (ASTM 2008a).

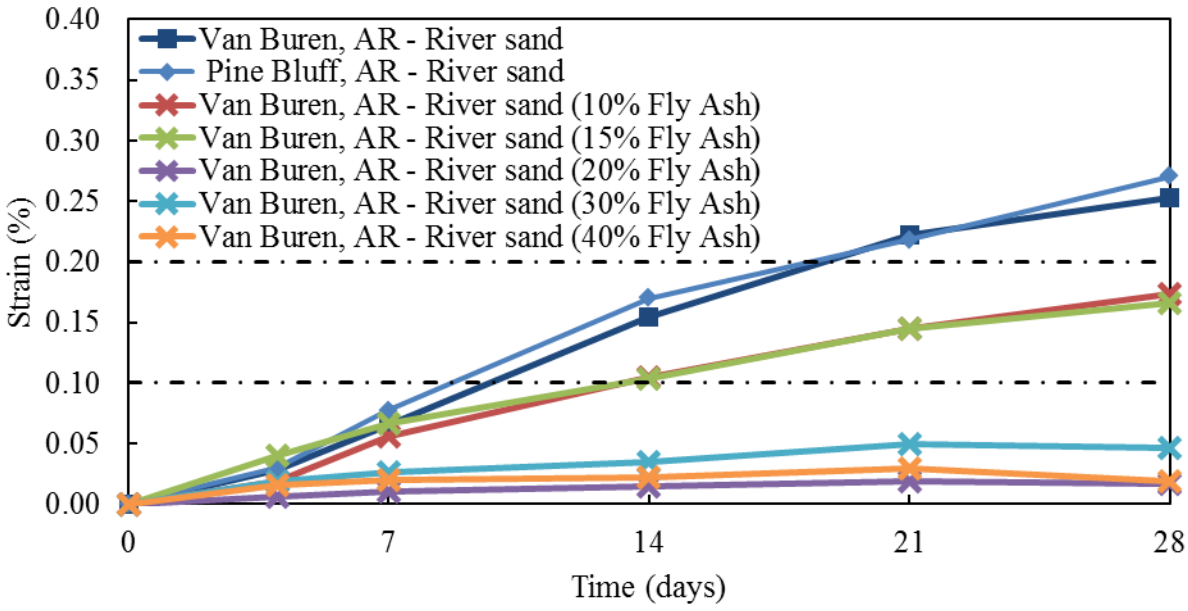

Figure 3.5. Strain (%) with respect to time (days) results for ASTM C1567 tests.

Pine Bluff (PB) – Mortar bars which contained river sand from Pine Bluff, Arkansas exhibited a similar high strain rate at the end of 16 days. Therefore, an additional test with an extended duration of 28 days was performed. The 28 day expansion was 0.27 percent, which indicated 'deleterious expansion.' Aggregate from Van Buren, AR and Pine Bluff, AR are similar and both are dredged from the Arkansas River. Therefore, aggregate from Van Buren was tested with fly ash and the results are applicable to aggregates from either Van Buren or Pine Bluff.

Van Buren with Fly Ash - To determine the minimum cement replacement rate with fly ash which prevents ASR, according to ASTM C1567, in concrete containing river sand from Van Buren, Arkansas, several replacement rates of Class C fly ash were evaluated. As shown in Figure 3.5, mortar bars which contained a replacement of 10 or 15 percent cement by weight with fly ash developed a 28 day expansion of 0.17 percent. However, when a replacement rate of 20 percent was used, the 28 day expansion was only 0.016 percent, and the combination was classified as 'inert.' As shown in Figure 3.5, mortar bars with 30 and 40 percent fly ash developed 28 day expansions of 0.046 and 0.018 percent, respectively. These results aggree with the replacement rate of 30 to 40 percent Class C fly ash which is typically recommended for the prevention of ASR (Thomas, 1995; Shehata & Thomas, 2000). Therefore, a replacement of fly ash, greater than 20 percent, will provide an 'inert' mixture. The ASTM C1567 test method is unreliable when evaluating fly ash as a preventative measure. Therefore, long term CPT and/or outdoor exposure tests are necessary to validate the results.

3.3 Field Monitoring

Strain and internal relative humidity were monitored for one year in the 15 median barrier sections. There were five sections each of minimal, moderate, and severe damage. The strain

data was presented with percent strain on the ordinate axis and days on the abscissa. The strain, relative humidity, and temperature data were plotted separately for each damage level. Monitoring began on January 31, 2013 and the treatments were applied March 12, 2013. The final measurements were conducted on January 14, 2014.

3.3.1 Temperature Normalized Strain Results

The ambient temperature varied between 0 and 30 degrees Celsius during monitoring of the median barrier. The ambient temperature at the time of initial measurements was 5 degrees Celsius and increased to 28 degrees Celsius by 161 days. Due to the variation in ambient temperature and the relatively high coefficient of thermal expansion (CTE) of concrete, the strain data was normalized to a standard temperature of 24 degrees Celsius. A CTE of 10×10^{-5} in/in per degree Celsius was used when normalizing the strain data. The raw data, prior to temperature normalization, is summarized in Appendix A1.4. The temperature normalized data for median barrier sections are summarized in Figure 3.6 for sections of minimal damage, Figure 3.8 for sections with moderate damage, and Figure 3.10 for sections of severe damage. The data for each section is labeled with the applied treatment and an alpha-numeric code for quick reference.

To compare the efficacy of each treated section to the untreated control section, the differential strain for each treated median barrier section was determined. The differential strain was determined by subtracting the temperature normalized strain of the control section from that of each corresponding treated section. The temperature normalized differential strain data for median barrier sections are summarized in Figure 3.7 for section with minimal damage, Figure

3.9 for sections of moderate damage, and Figure 3.11 for sections with severe damage. Again, the data for each section is labeled with the applied treatment and an alpha-numeric code.

To describe the efficacy of each treatment in reducing strain over time, the strain rate for each median barrier section was also determined. The strain rate is a statistical approximation of the linear trend of the strain data. The intercept of each linear trend was forced through the origin, to include zero strain which must occur at the beginning of monitoring. The R^2 value for each linear trend line was also determined. The strain rate linear trend lines for each damage level are summarized in Appendix A1.3. The strain rate for the differential strain was determined in the same manner. The strain rates are summarized as percent per year. The differential strain rate also provides a comparison of the efficacy of each treated section with respect to the untreated control section. The strain rate data for median barrier sections are summarized below in Table 3.2 for section of minimal damage, Table 3.3 for sections of moderate damage, and Table 3.4 for sections of severe damage.

3.3.1.1 Minimal Damage

As shown in Figure 3.6, the median barrier sections of minimal damage exhibited one-year strains in the range of 0.0016 to 0.0158 percent. The one-year strain in sections of minimal damage was less than the 0.04 percent strain required to produce visible cracking in unreinforced concrete (Ideker et al., 2012a). Section S-1 had the greatest strain for sections of minimal damage, and section L-1 had the least. Section S-1 had more strain than section C-1 throughout the duration of monitoring. Section L-1 exhibited less strain than that of section C-1 and even contracted between 126 and 259 days. Section EP-1 also exhibited less strain than section C-1 and developed the second greatest reduction in strain. Section S2-1 exhibited strain similar to

that of section C-1 until the second application of silane. After the second treatment, the strain in section S2-1 decreased below that of section C-1.

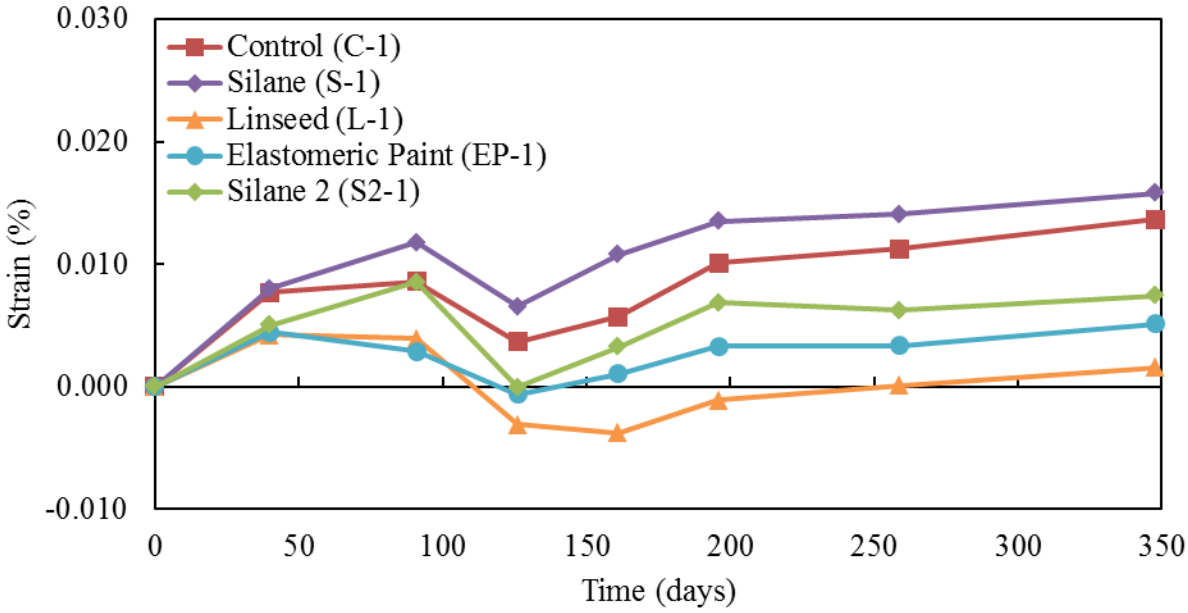

Figure 3.6. Temperature normalized vertical strain (%) with respect to time (days) results for median barrier sections which exhibit minimal damage.

As stated above, strain rate represents a statistical approximation of a linear trend within the strain data. The provided R^2 data represents the standard error between the data and the linear trend. In addition, the linear trend was forced through the origin to provide zero strain at the beginning of monitoring. The strain rate data for sections of minimal damage were summarized in Table 3.2. The strain rate of section C-1 was 0.0159 percent per year. As stated earlier, a strain greater than 0.04 percent will produce visible cracking within concrete. At the current strain rate, visible cracking will develop in sections of minimal damage within 2.5 years. Section S-1 exhibited a higher strain rate than section C-1, while section L-1 exhibited the lowest strain rate at -0.0001 percent per year. However, there was variability in the data for L-1, and the R^2 value was only 0.0006. Between 196 days and one-year, the strain rate of section L-1 increased

to provide a one year strain of 0.0016 percent. Section EP-1 also exhibited a low strain rate as compared to that of section C-1. However, the section developed a one year expansion of 0.0051 percent. Section S2-1 exhibited a lower strain rate than section C-1 and slowed between 196 days and one-year. The one year strain in sections S2-1 was 0.0075 percent.

Table 3.2. Strain rates for temperature normalized vertical strain in median barrier sections with minimal damage.

Section	Strain Rate	R^2	[a]Differential	R^2
	%/Yr.		%/Yr.	
Control (C-1)	+0.0159	0.8877	--	1.0000
Silane (S-1)	+0.0207	0.8973	+0.0048	0.6871
Linseed (L-1)	-0.0001	0.0006	-0.0160	0.9511
Elastomeric Paint (EP-1)	+0.0050	0.6786	-0.0109	0.9328
Silane 2 (S2-1)	+0.0093	0.7126	-0.0066	0.9110

[a]Differential strain rate between treated section and control section

The same trends were apparent in Figure 3.7, which shows the differential strain for sections of minimal damage. The differential strain is the difference in strain between the untreated control sections and each respective treated section. The differential strains show that, with the exception of section S-1, all the surface treatments provide a reduction in strain as compared to section C-1. Sections L-1 and EP-1 developed the largest reductions in strain as compared to section C-1. However, Section S2-2 exhibited a decreasing strain rate between 196 days and one-year. From the current trend, the strain in section S2-1 will decrease below that of section EP-1 within six months.

Boiled linseed oil, elastomeric paint, and two applications of silane provided a reduction in strain for sections of minimal damage. Two applications of silane provided a decreasing strain rate during the winter, which suggest the strain will continue to decrease as compared to the control section. However, a single application of silane was not sufficient to provide a reduction in

strain as compared to the control. Elastomeric paint also reduced strain as compared to the control, although it is much more demanding to apply. Boiled linseed oil provided the most promising reduction in strain for sections of minimal damage and is an effective alternative treatment method. However, it does not provide a breathable vapor barrier between the concrete and air, and will trap excess moisture within the concrete. Applying the boiled linseed oil after a period of low ambient humidity will trap less moisture within the concrete.

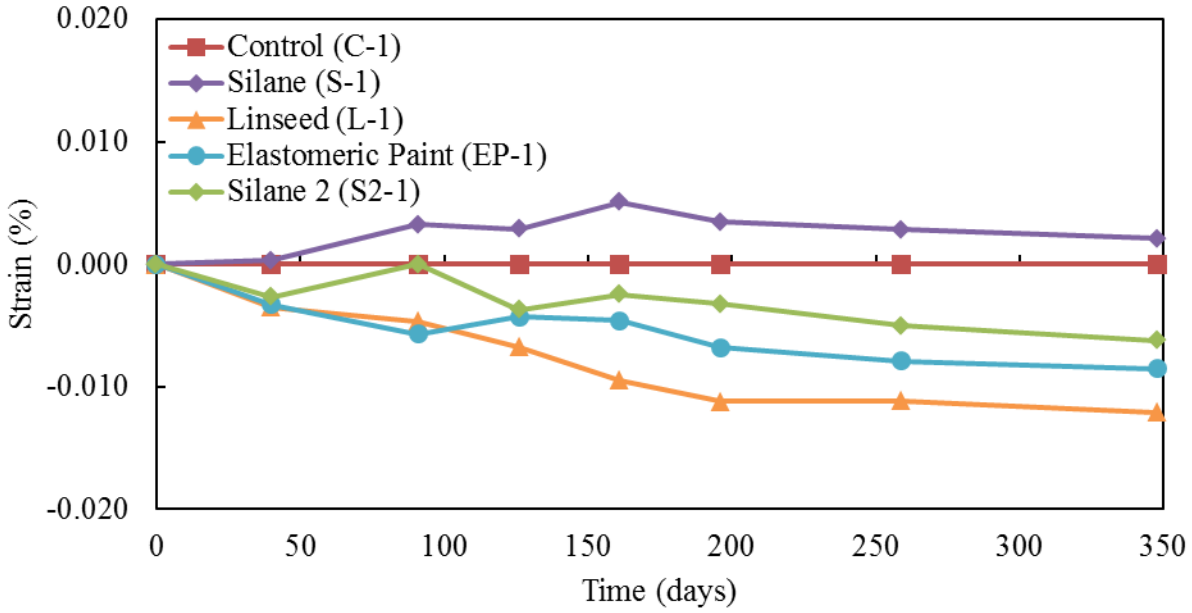

Figure 3.7. Differential vertical strain (%) with respect to time (days) results for median barrier sections which exhibit minimal damage.

3.3.1.2 Moderate Damage

From Figure 3.8, the median barrier sections of moderate damage exhibited one-year strains in the range of 0.03 to 0.046 percent. Therefore, strains which will produce visible cracking occur within one year in most of the sections which exhibit moderate damage. The treatments did not reduce strain in sections of moderate over the course of monitoring. Section EP-2 experienced a

reduction in strain between 91 and 259 days; however, the increase in strain between 259 days and one year was larger than that of section C-2. Section L-2 exhibited a similar large increase in strain between 259 days and one-year, and exhibited the greatest strain at one-year. The increase in strain for sections EP-2 and L-2 may be attributed to freezing and thawing damage which occurred during the winter. However, sections C-2, S-2 and S2-2 did not exhibit the same level of strain between 259 days and one year. Therefore, the silane may have provided some benefit as compared to the other treatments. Silane did not provide a benefit as compared to the untreated section C-2. Section S-2 exhibited lower stain than that of section C-2 throughout the duration of monitoring, and the strain in section S-2 was lower than that of section C-2 between 40 and 161 days. The strain remained lower than that of section C-2 due in part to the low strains which occurred soon after treatment.

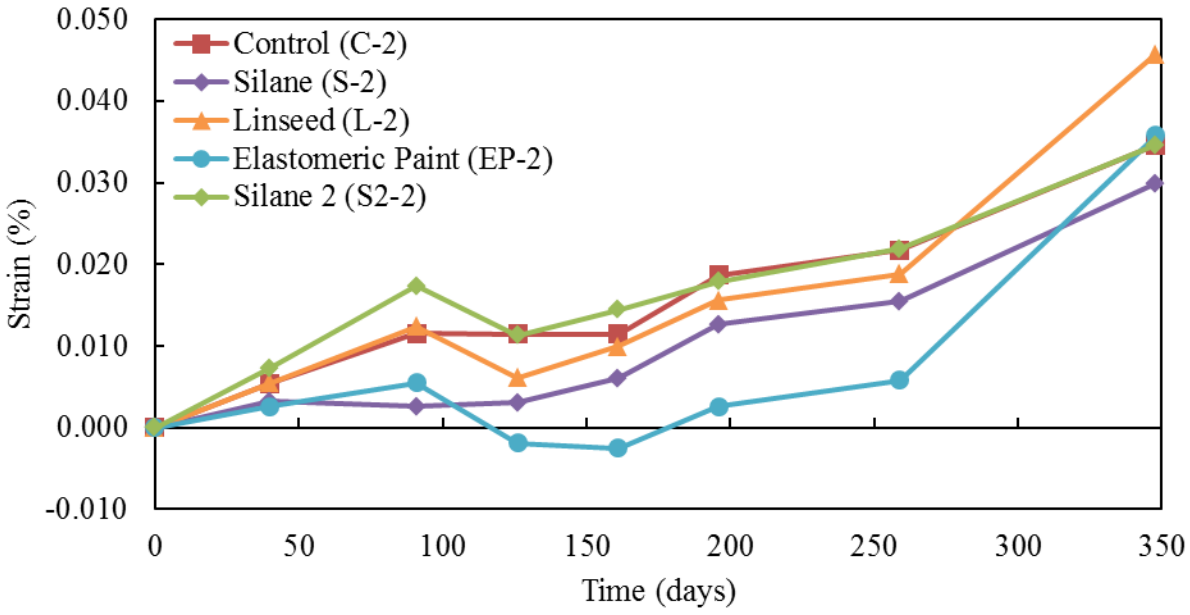

Figure 3.8. Temperature normalized vertical strain (%) with respect to time (days) results for median barrier sections which exhibit moderate damage.

However, section S2-2 exhibited greater or equal strains to section C-2 between 40 and 161 days and did not react to the first treatment. The strain in section S2-2 exhibited a small benefit from the second application of silane at 161 days. However, the reduction was not enough to reduce the strain in section S2-2 below that of section C-2. One possible explanation for the limited effectiveness of treatments on sections of moderate damage is the level of surface cracking. The cracks were too narrow to effectively fill with a silicon sealer, which left avenues for water to enter the concrete, exacerbating both ASR and freezing and thawing deterioration.

The strain rate data for sections of moderate damage are summarized in Table 3.3. The strain rate of section C-2 was 0.0339 percent per year, which is roughly twice that of section C-1. Therefore, the damage classification of sections based on visible distress effectively differentiated between sections of minimal and moderate damage. The strain rates for all treated sections were within 0.0150 percent per year of the strain rate for section C-2.

Table 3.3. Strain rates for temperature normalized vertical strain in median barrier sections with moderate damage.

Moderate Damage	Strain Rate	R^2	[a]Differential	R^2
	%/Yr.		%/Yr.	
Control (C-2)	+0.0339	0.9853	--	1.0000
Silane (S-2)	+0.0244	0.9175	-0.0095	0.6745
Linseed (L-2)	+0.0362	0.9076	+0.0022	0.0592
Elastomeric Paint (EP-2)	+0.0189	0.5470	-0.0150	0.5075
Silane 2 (S2-2)	+0.0352	0.9631	+0.0013	0.0720

[a]Differential strain rate between treated section and control section

The section EP-2 stain data had an R^2 value of 0.55. Until 259 days, the strain rate in section EP-2 was lower than that of section C-2. However, between 259 days and one-year the strain rate increased. Again, this change is likely due to freezing and thawing damage. Although section EP-2 developed a one-year strain close to that of the section C-2, the strain rate was only

0.0189 percent, due to the low strains which occurred between 126 and 259 days. Sections L-2 and S2-2 had similar strain rates to that of section C-2. The strain rate in section L-2 was similar to that of section C-2 until 259 days, at which point the strain increased. The strain rate in section S-2 was lower than that of C-2 and a single application of silane provided some benefit as compared to the control. Interestingly, a single application of silane provided a limited reduction in expansion, while section S2-2 did not benefit from two applications of silane.

From the differential strains in sections of moderate damage, as shown in Figure 3.9, only sections S-2 and EP-2 exhibited a reduction in strain as compared to section C-2. Sections S2-2 exhibited no differential strain between 161 days and one year. Sections EP-2 and L-2 exhibited a large differential strain between 259 days and one year.

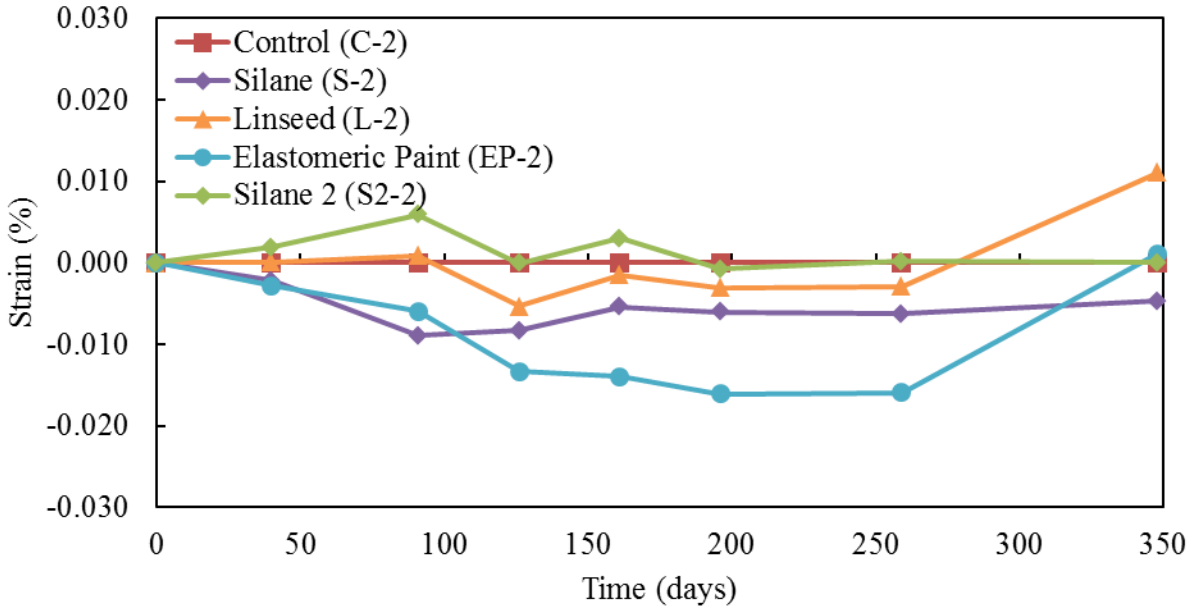

Figure 3.9. Differential vertical strain (%) with respect to time (days) results for median barrier sections which exhibit moderate damage.

Another explanation for the increase in strain between 259 days and one-year is moisture trapped by the surface treatment which could not escape during freezing, and produced more freezing

and thawing damage than untreated section and sections which allowed moisture to escape quickly during freezing. Sections EP-2 was the only section of moderate damage which observed a reduction in ASR related strain, with a decrease in differential strain between 91 and 259 days. Section S-2 also experienced a limited reduction in strain as compared to section C-2, however, the differential strain was only 0.0047 percent below that of the control at one-year.

Elastomeric paint and a single application of silane were the only treatments which reduced ASR related strains for sections of moderate damage. The sections treated with two applications of silane or linseed oil did not show any benefit from treatment. The sections treated with linseed oil and elastomeric paint developed strains during the winter and fared worse than the untreated control section when exposed to freezing and thawing distress. The sections of moderate damage require better crack filling to allow the surface treatments to work effectively. However, a silicon crack sealer did not adequately fill fine cracks, and a low viscosity epoxy is likely better suited to fill narrow cracks.

3.3.1.3 Severe Damage

As shown in Figure 3.10, the median barrier sections of severe damage exhibited one-year strains in the range of 0.037 to 0.103 percent. Strains which produce additional cracking continued to occur even in the treated sections. The greatest increase in strain for median barrier sections of severe damage occurred between 259 days and one-year. This coincides with winter weather and the increase in strain was likely due to freezing and thawing related distress. Section C-3 exhibited a one-year strain of 0.095 percent, which is higher than that of sections of minimal and moderate damage. Sections S-3, L-3, and S2-3 all experienced a reduction in strain as compared to sections C-3. At 161 days, a second application of silane was applied to section S2-3, and

section S2-3 continued to exhibit less strain than the other treated sections. The final strain in section S2-2 was 0.037 percent. Section S-3 exhibited greater strain than that of section C-3 between 0 and 161 days and then the strain decreased below that of section C-3 until one-year. The strain in section EP-3 closely followed that of section C-3 throughout one-year. Section EP-3 had greater strain than section C-3, and had the largest increase in strain between 259 days and one-year. The cracks in the sections of severe damage were too wide for elastomeric paint to bridge, and the silicon crack sealer used to fill the large cracks did not provide adequate moisture protection.

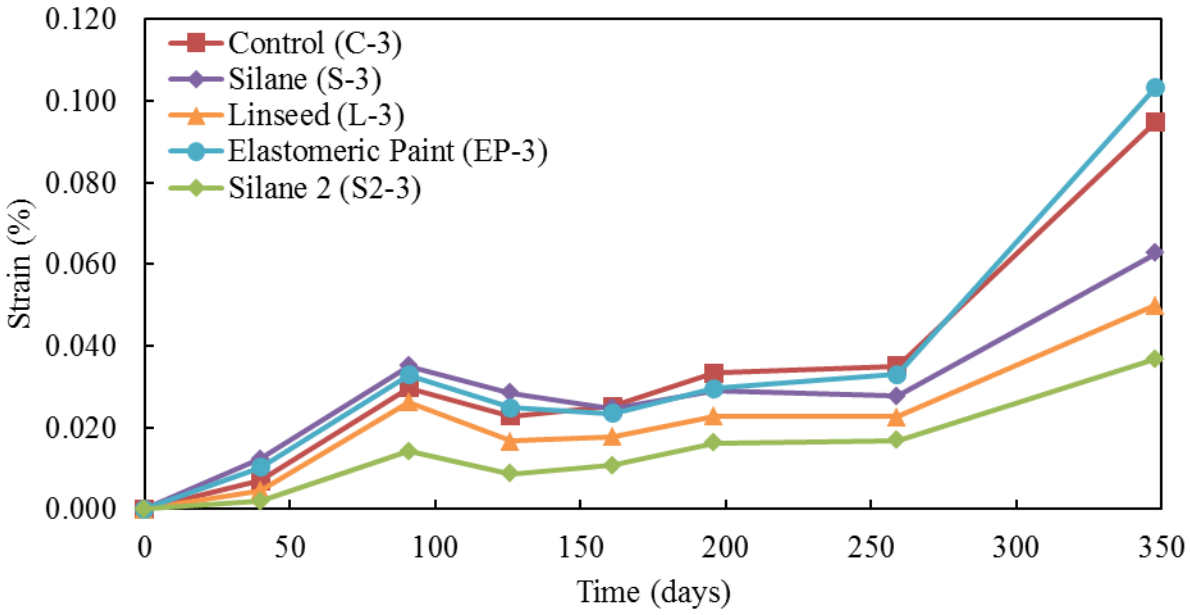

Figure 3.10. Temperature normalized vertical strain (%) with respect to time (days) results for median barrier sections which exhibit severe damage.

The strain rate data for sections of severe damage are summarized in Table 3.4. The strain rate of section C-3 was 0.0767 percent per year, which was roughly two times that of section C-2, and 5 times that of section C-1. Again, the damage classification of sections based on visible distress effectively differentiated between sections of minimal, moderate, and severe damage.

The strain rate of section EP-3 was higher than that of section C-3, and the R^2 value for section EP-3 was 0.88. The strain in section EP-3 had very little variability until 259 days, at which point the strain increased rapidly. The other sections of severe damage had R^2 values greater than 0.91, and showed little variability until 259 days. The strain rate in section S2-3 was less than half that of section C-3, and section S2-3 clearly provided the greatest reduction in strain as compared to section C-3. Section L-3 also exhibited a reduction in strain as compared to section C-3; however, the strain rate did not decrease below that of section C-3 until 161 days. Meanwhile, Section S-3 exhibited a greater strain rate than that of section C-3 until 161 days, at which point the strain in section S-3 decreased below that of section C-3.

Table 3.4. Strain rates for temperature normalized vertical strain in median barrier sections with severe damage.

Severe Damage	Strain Rate	R^2	[a]Differential	R^2
	%/Yr.		%/Yr.	
Control (C-3)	+0.0767	0.9172	--	1.0000
Silane (S-3)	+0.0602	0.9092	-0.0165	0.4770
Linseed (L-3)	+0.0462	0.9248	-0.0305	0.8128
Elastomeric Paint (EP-3)	+0.0795	0.8803	+0.0028	0.1348
Silane 2 (S2-3)	+0.0323	0.9427	-0.0445	0.8884

[a]Differential strain rate between treated section and control section

The differential strains in sections of severe damage are summarized in Figure 3.11. Only section EP-3 increased in strain as compared to section C-3. Sections S2-3 had a reduction in differential strain as compared to section C-3, and the final strain in section S2-3 was 0.058 percent lower than that of section C-3. Section L-3 also exhibited lower strain than section C-3. However, section L-3 took longer to develop a reduction in strain as compared to section C-3. Both sections EP-3 and S-3 had higher strains than section C-3 until 161 days. After 161 days, the strain in section S-3 decreased to a level lower than that of C-3, while the strain in section

EP-3 increased. Similar to section EP-2, the strain in section EP-3 increased between 259 days and one-year. This is again likely due to freezing and thawing damage, rather than ASR. The cracks in sections of severe damage were not bridged by the elastomeric paint. Therefore, moisture entered the concrete and was not able to escape during freezing. Section C-3 also exhibited freezing and thawing damage. However, sections S-3, L-3, and S2-3 did not exhibit the same level of strain between 259 days and one-year. Section S2-3 reacted much better with an additional application of silane to protect from water ingress.

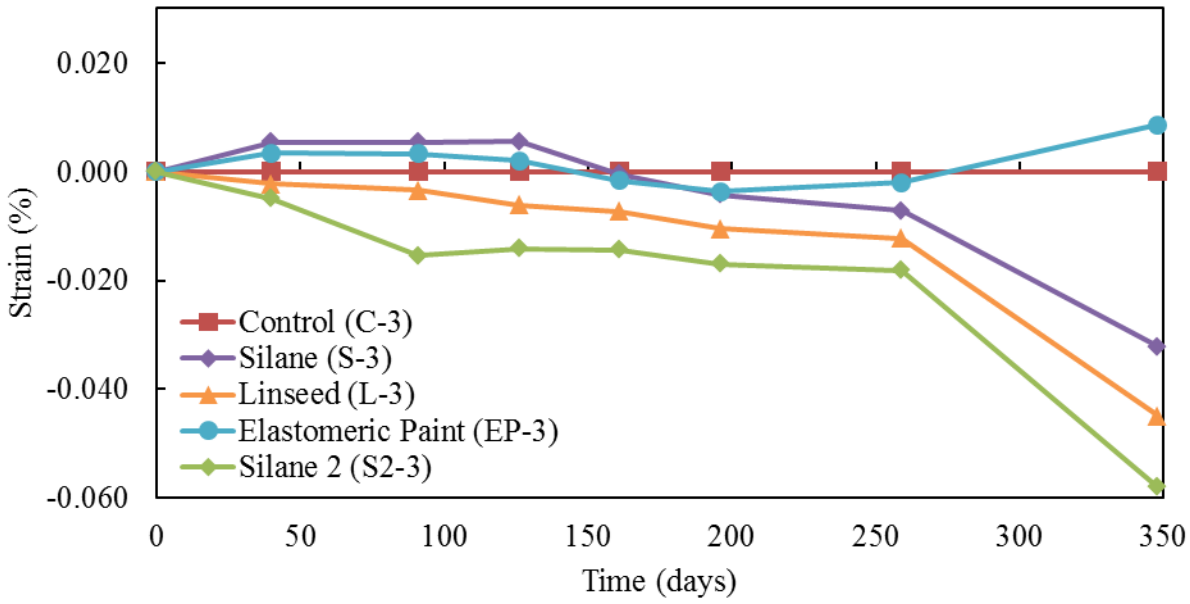

Figure 3.11. Differential vertical strain (%) with respect to time (days) results for median barrier sections which exhibit severe damage.

One possible explanation for the performance of silane and linseed oil sealers is the low viscosity, which allows the sealers to enter large cracks and seal the internal surfaces of the crack. Therefore, the concrete is protected from the ingress of additional moisture although cracking still exists. In contrast, the elastomeric paint has a higher viscosity and does not enter the cracks to seal the additional surface area. Again, the use of a low viscosity crack injection

before the application of surface treatments would allow sealant to fill some of the larger cracks. Two applications of silane provided a beneficial decrease in strain related to ASR without additional crack sealant.

3.3.2 Internal Relative Humidity and Temperature Results

Internal relative humidity and temperature were measured using a portable probe during each monitoring visit. The internal relative humidity and temperature data were summarized for each damage level and compared to the ambient conditions. The internal relative humidity data is shown in Figure 3.12 for sections of minimal damage, Figure 3.14 for moderate damage, and Figure 3.16 for severe damage. The temperature data is shown in Figure 3.13 for sections of minimal damage, Figure 3.15 for moderate damage, and Figure 3.17 for severe damage. The relative humidity is shown in percent, and time in days. The data for each section is labeled with the applied surface treatment and an alpha-numeric code. The relative humidity data was not normalized, and represents the internal relative humidity at the ambient temperature. There was concern that moisture entered the humidity ports between measurements and allowed the relative humidity to increase above the levels within the concrete. However, there were some fluctuations in the relative humidity, particularly in sections of minimal damage, which are worth noting. If the internal relative humidity in the median barrier is reduced below 85 percent, ASR will slow or arrest.

3.3.2.1 Minimal Damage

The internal relative humidity data for sections of minimal damage are summarized in Figure 3.12. The fluctuations in internal relative humidity for section C-1 did not follow the ambient conditions, and was roughly 25 percent greater than ambient relative humidity. The internal

relative humidity of section S-1 closely followed that of section C-1 until the ambient relative humidity decreased after 161 days. The internal relative humidity of section S-1 decreased to 81.4 percent as compared to section C-1 where the internal relative humidity remained at 98.5 percent. The internal relative humidity in section S-1 remained below that of section C-1 until one year, at which point the internal relative humidity increased to 95.4 percent. Therefore, during the summer months the silane surface treatment reduced internal relative humidity to a level where ASR was slowed. The internal relative humidity of section L-1 closely followed that of section C-1 throughout one-year.

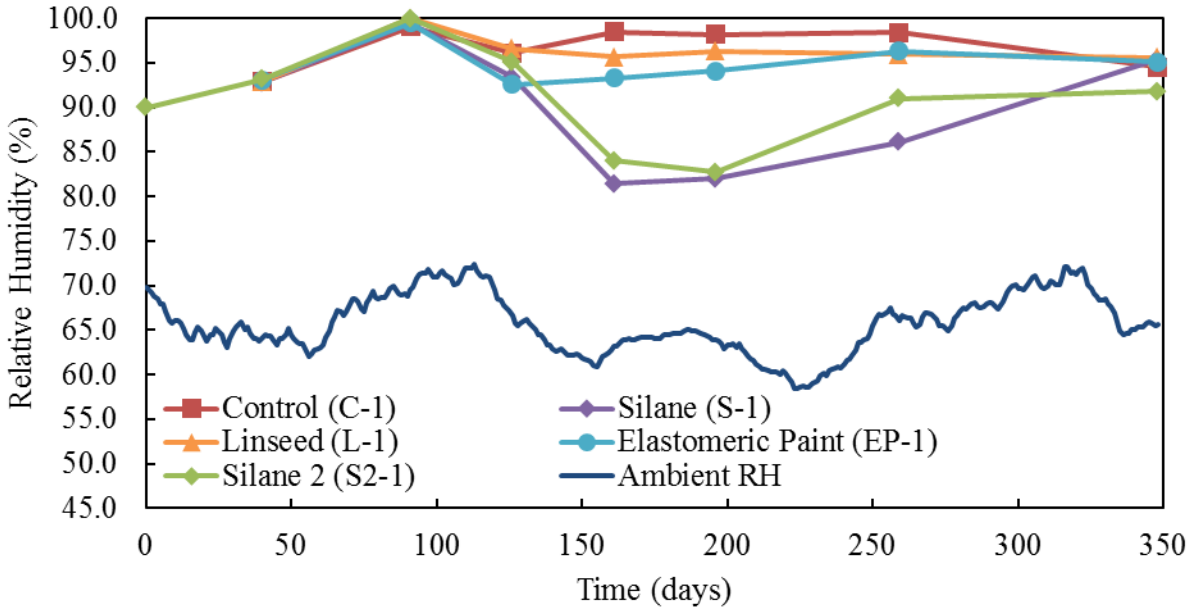

Figure 3.12. Internal relative humidity (%) with respect to time (days) results for median barrier sections which exhibit minimal damage.

The internal relative humidity of section L-1 decreased slightly, after 161 days, to 95.7 percent. However, the internal relative humidity of section L-1 increased at one-year and was slightly higher than that of section C-1. Section EP-1 provided some insulation from temperature fluctuations, and the internal relative humidity decreased to 93.3 percent at 161 days. The

internal relative humidity of section EP-1 returned to 95.1 percent at one year. The internal relative humidity of section S2-1 followed that of section C-1 until 161 days at which point the internal relative humidity decreased to 84 percent. Similar to section S-1, two application of silane was able to reduce the internal relative humidity below 85 percent and slow the ASR. The internal relative humidly of section S2-1 remained lower than that of section C-1 until 259 days, at which point the internal relative humidity increased to 91 percent. The sections treated with silane were the only sections of minimal damage to witness a reduction in internal relative humidity as compared to section C-1. During the summer, the humidity in sections S-1 and S2-1 decreased to 81.4 and 82.7 percent, respectively. At the same time the ambient humidity decreased from 72.4 to 58.6 percent which explains the decrease in relative humidity.

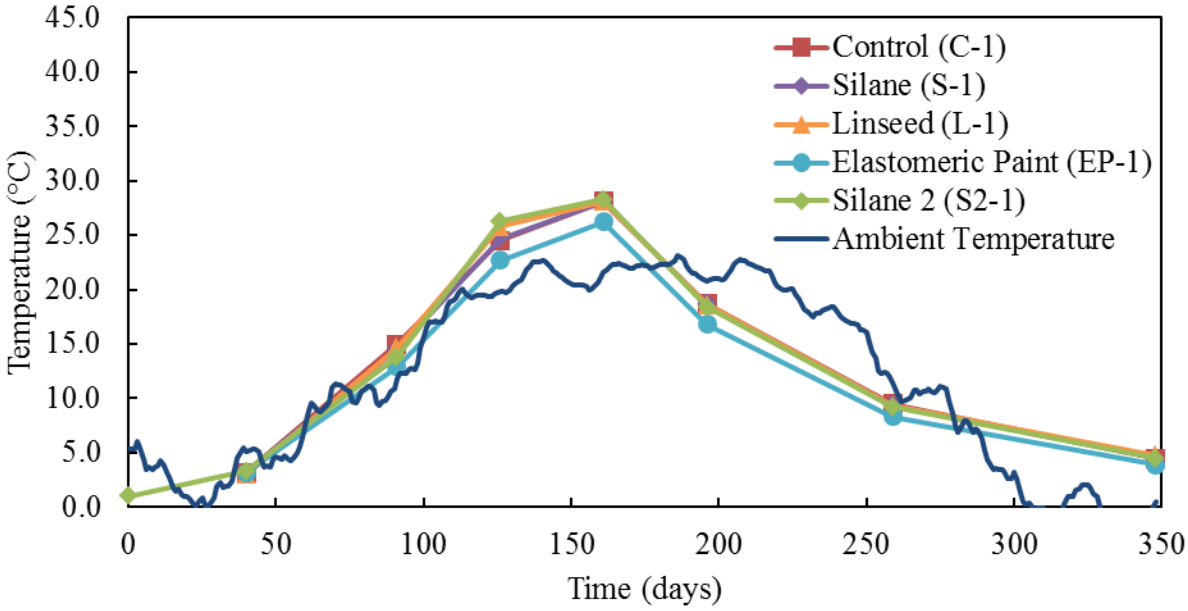

Figure 3.13. Internal temperature (°C) with respect to time (days) results for median barrier sections which exhibit minimal damage.

The internal temperature data for sections of minimal damage is summarized in Figure 3.13. With the exception of section EP-1, the internal temperature of sections of minimal damage

followed the ambient conditions throughout the year. The internal temperature of section EP-1 was roughly 2 degrees Celsius lower than that of section C-1 due to the insulating properties of the treatment.

Silane reduced the internal relative humidity below 85 percent during the summer months. As stated earlier, the moisture within the concrete was mobile and was pulled toward the surface of the concrete when a humidity gradient developed between the concrete and air. The silane treatment is breathable and allowed some of the internal humidity to escape. However, when the ambient humidity increased during the winter, there was less of a humidity gradient and the moisture within the concrete returned to the core. Therefore, an increase in relative humidity was measured. The elastomeric paint was also breathable and produced a humidity gradient between the concrete and air, and a small decrease in internal relative humidity was measured. Linseed oil is not breathable and no decrease in internal relative humidity was measured.

3.3.2.2 Moderate Damage

The internal relative humidity data for sections of minimal damage is summarized in Figure 3.14. The internal relative humidity for section C-2 varied between 89.2 and 99.4 percent, and the internal relative humidity for section C-2 was 95.2 percent at one-year. The internal relative humidity of section S-2 closely followed that of section C-2, and the internal relative humidity for section S-2 decreased to 94.1 percent at one-year. The internal relative humidity in section L-2 followed that of section C-2, with a one-year internal relative humidity of 94.8 percent. The only fluctuations in internal relative humidity for section L-2 occurred at 161 and 196 days of monitoring. The internal relative humidity for section EP-2 followed that of section C-2 until 259 days, at which point the internal relative humidity of section EP-2 increased to 96.9 percent

by one year. The internal relative humidity achieved a minimum of 95.2 percent at 126 days. The internal relative humidity in section S2-2 was similar to that of section S-2. The internal relative humidity in section S2-2 decreased to a level below that of section C-2 after 196 days of monitoring and remained below throughout one-year, and the internal relative humidity for section S2-2 was 94.0 percent at one-year.

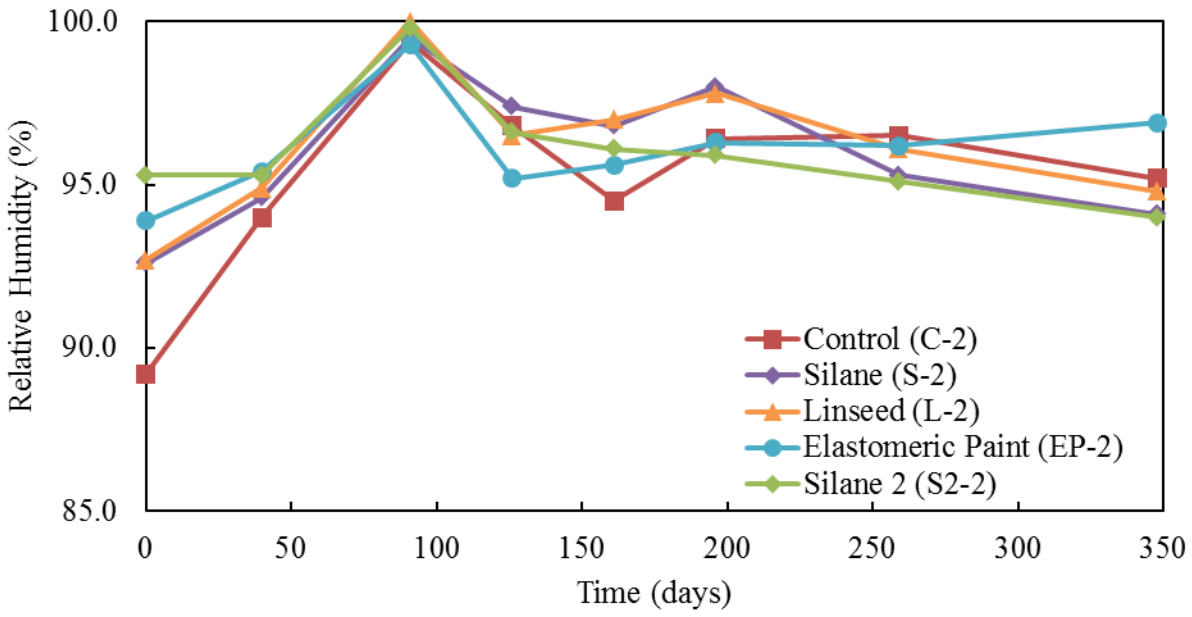

Figure 3.14. Internal relative humidity (%) with respect to time (days) results for median barrier sections which exhibit moderate damage.

The temperature data for sections of moderate damage are summarized in Figure 3.15. The temperatures again followed the ambient conditions, with the exception of section EP-2. The temperature profile of section EP-2 was ~2 degrees Celsius lower than that of section C-2 due to the insulating properties of elastomeric paint and its reflective color.

The silane treated sections of moderate damage exhibited a small decrease in internal relative humidity as compared to the control section at one-year. However, due to the extensive cracking

in the sections of moderate damage none of the treatments reduced internal relative humidity over the course of monitoring. Again a better method for filling cracks before treatment would allow the surface treatments to produce a humidity gradient which pulls moisture out of the concrete. None of the surface treatments reduced internal relative humidity below 85 percent, and ASR continued.

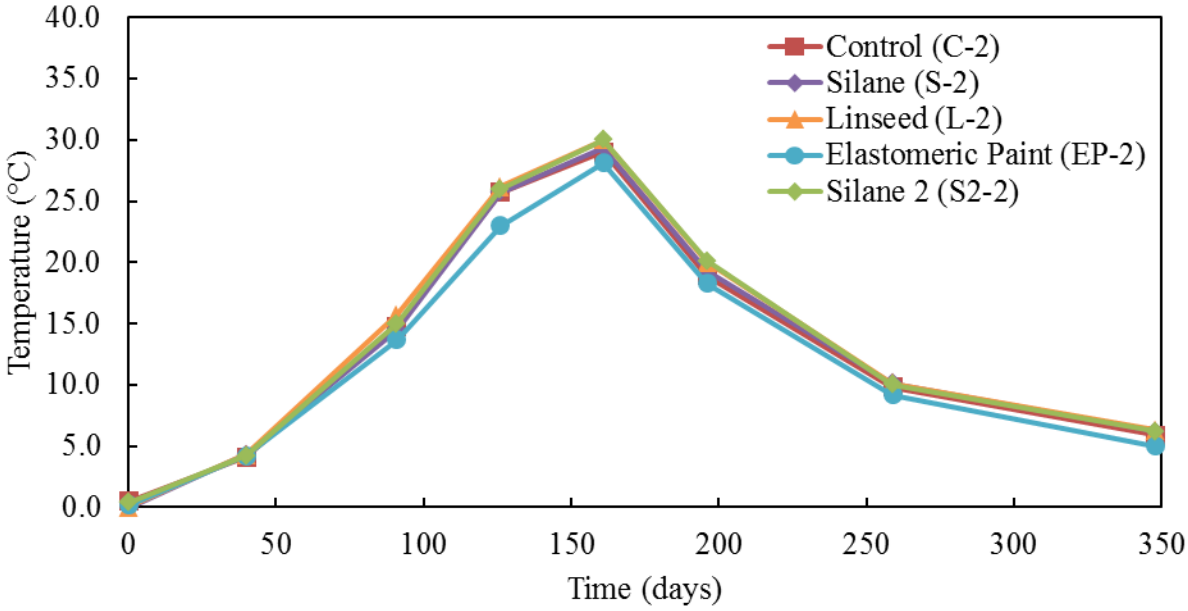

Figure 3.15. Internal temperature (°C) with respect to time (days) results for median barrier sections which exhibit moderate damage.

3.3.2.3 Severe Damage

The internal relative humidity data for sections of severe damage were summarized in Figure 3.16. The internal relative humidity for section C-3 varies between 90.9 and 99.7 percent, and the internal relative humidity of section C-3 was 95.8 percent at one year of monitoring. The internal relative humidity of section S-3 closely followed that of section C-3, and the relative humidity for section S-3 was 96.4 percent at one year of monitoring. The internal relative

humidity in section L-3 followed that of section C-3, with a one year internal relative humidity of 97.7 percent. The internal relative humidity for section EP-3 was lower than that of section C-3 between 91 and 259 days of monitoring. However, the internal relative humidity for section EP-3 was 97.6 percent at one year. The internal relative humidity of section EP-3 achieved a minimum of 95.0 percent at 161 days of monitoring. The internal relative humidity in section S2-3 was similar to that of section C-3, although the internal relative humidity for section S2-3 was 97.6 percent at one year, which was higher than that of section C-3.

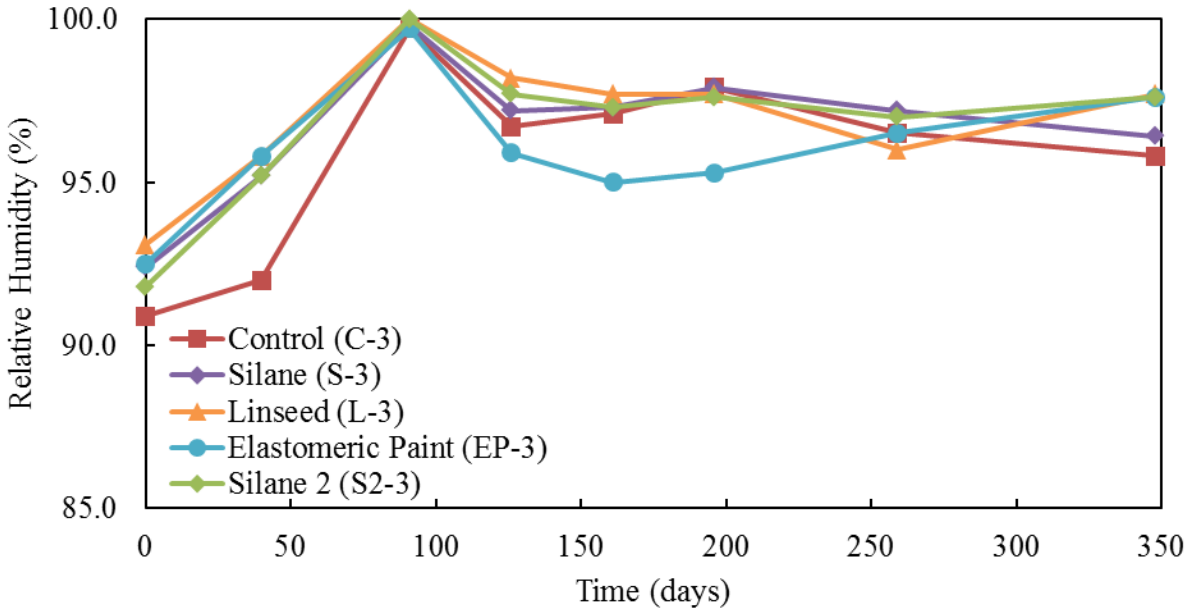

Figure 3.16. Internal relative humidity (%) with respect to time (days) results for median barrier sections which exhibit severe damage.

The internal temperature data for sections of severe damage are summarized in Figure 3.17. The temperature profiles again followed the ambient conditions with the exception of section EP-3. The temperature profile of section EP-3 was again ~2 degrees Celsius lower than that of section C-3 due to reflectivity of the white elastomeric paint.

Similar to the sections of moderate damage, the sections with severe damage exhibited cracks which were not adequately filled with silicon sealer. Therefore, no decrease in internal relative humidity was measured in any of the sections, with the exception of the sections treated with elastomeric paint. During the summer months, the elastomeric paint formed a relative humidity gradient between the concrete and air which pulled moisture from the concrete. Therefore, a small decrease in relative humidity was measured. However, the other treatments did not provide a reduction in internal relative humidity because the cracks were not adequately sealed. Again, none of the surface treatments reduced internal relative humidity below 85 percent.

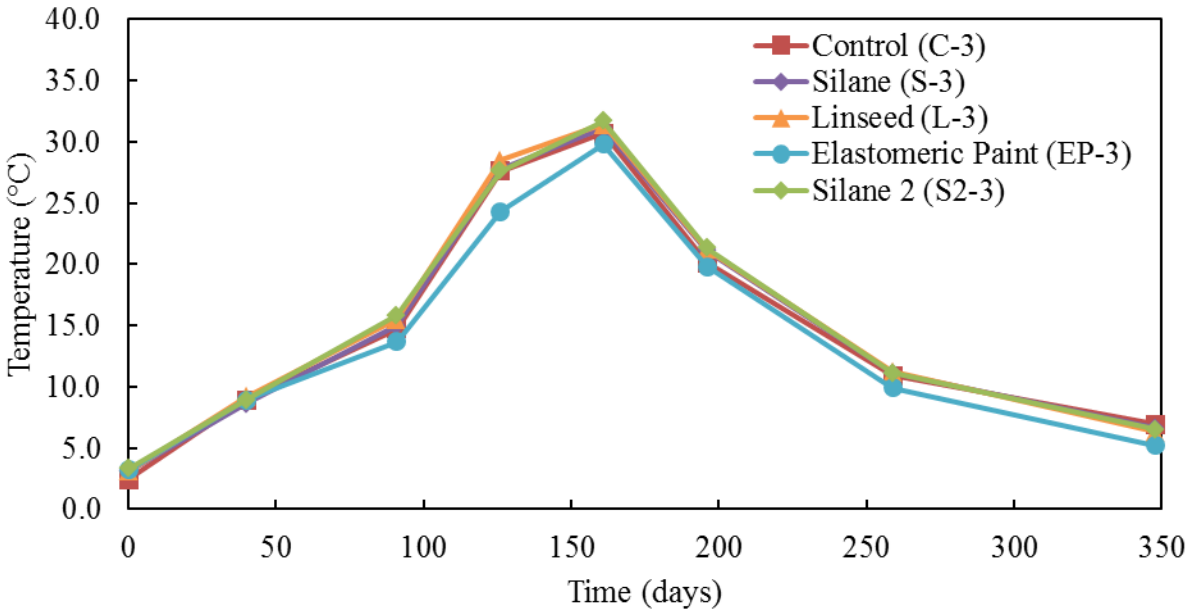

Figure 3.17. Internal temperature (°C) with respect to time (days) results for median barrier sections which exhibit severe damage.

3.3.2.4 Note on Internal Relative Humidity and Temperature

There was concern that moisture entered the humidity monitoring ports from the ambient environment and invalidated the results. Due to the very high relative humidity measured even at temperatures greater than 24 degrees Celsius, normalization of the data was not possible. It

was also apparent from the very high internal relative humidity measured throughout the year, that external moisture must have entered the humidity ports to allow the humidity to remain constant as the temperature increased. A better system of protecting the humidity ports from external moisture is required.

4 Recommendations and Conclusions

4.1 Conclusions from Laboratory Testing

A petrographic analysis of concrete from the median barrier found evidence of ASR which was associated with the coarse portion of the fine aggregate. Tests showed the river sand contained chert and chalcedony minerals, which reacted with the high alkali pore solution to form alkali-silica deposits and microcracking. The microcracking allowed excess moisture to enter the concrete, which lead to the development of freezing and thawing deterioration.

Arkansas River sand from Van Buren Arkansas developed a 14 day expansion greater than 0.10 percent during the AMBT, and the sand was categorized as potentially deleteriously reactive, which confirms the findings of the petrographic analysis. The CPT results classify Arkansas River sand as inert, which contradicts the results of the AMBT and petrographic analysis. However, the results of the CPT were possibly a false negative due to alkali leaching which occurred during storage of the prisms. The CPT standard provides recommendations on limiting alkali leaching which are essential. Unfortunately there was not sufficient time to evaluate an additional sample of the aggregate. However, AMBT and petrographic analysis of samples containing the same aggregate conclude that the aggregate will lead to the development of ASR.

The median barrier concrete contained high alkali cement and a low replacement of Class C fly ash. The development of ASR is due to the combination of the slowly reactive sand in addition to high alkali cement and a low replacement of fly ash. In addition, the variation in cement alkalis contributed to the variability in the damage present within the median barrier. The sections of minimal damage likely contained lower alkali cements than the sections of moderate or severe damage. The prevention of ASR in concrete which contains Arkansas River sand is

achieved through a combination of lower alkali cements and a higher replacement of Class C fly ash. Additional laboratory and outdoor exposure testing is required to determine the safe alkali level and fly ash replacement rate for concrete which contains Arkansas River sand.

4.2 Conclusions from Field Testing

A minimum of three years of monitoring is required to evaluate the efficacy of mitigation methods for ASR. Only one year of monitoring results are available from the median barrier. The trends which have become apparent within the first year are preliminary and do not reflect the final efficacy of each treatment method. However, some valuable information on the application and efficacy of each treatment, as well as necessary changes to the application methods, were observed.

All evaluated surface treatments provided a beneficial reduction in expansion for the sections of minimal damage. The boiled linseed oil provided the greatest reduction as compared to the control, while elastomeric paint was slightly less effective. The silane was not effective with a single application; however, a second application reduced expansion as compared to the control. As for limiting moisture ingress, only the sections treated with silane exhibited a reduction in internal relative humidity. The linseed oil treatment is not breathable and no reduction in moisture was expected. However, the elastomeric paint was not applied sufficiently to produce a breathable barrier. At the current strain rate, the sections of minimal damage will develop visible surface map cracking within 2.5 to 3 years. After map cracking develops, the freezing and thawing damage will accelerate and the median barrier will deteriorate to the point of moderate damage within a few years. Treating the sections of minimal damage with silane or boiled

linseed oil is recommended to prevent the ASR related deterioration from reaching the point of surface map cracking.

For the sections of moderate damage, only the elastomeric paint reduced expansion as compared to the control. Unfortunately, the sections treated with boiled linseed oil or elastomeric paint fared worse than the control section during the winter months. The sections of moderate damage suffered freezing and thawing damage during the winter. The boiled linseed oil and elastomeric paint likely trapped moisture in the concrete which exacerbated the damage as compared to the control. The silicon crack sealant was not sufficient to provide a water barrier on the concrete and none of the surface treatments provided a reduction in internal relative humidity for the sections of moderate damage. Again, treatment with two applications of silane will reduce freezing and thawing distress as long as the cracks are sealed prior to treatment.

The sections of severe damage exhibited much greater expansion than sections of minimal or moderate damage. However, silane and boiled linseed oil treatments proved effective at reducing expansion as compared to the control. The contrast in treatment effectiveness as compared to the sections of moderate damage is possibly explained by the lower viscosity of the sprayed treatments and the increased level of cracking in the section of severe damage. The treatments were able to enter the cracks and seal the surface of the additional concrete which provided some benefit during the summer and winter. Boiled linseed oil and two applications of silane provided the greatest reduction in expansion as compared to the control. Due to the presence of extensive map cracking and wide longitudinal cracks, none of the surface treatments provided a beneficial reduction in internal relative humidity for the sections of severe damage. Again, better crack sealant prior to treatment would provide an even greater reduction in expansion.

As discussed in the results from the petrographic analysis, the distress in the median barrier was caused from the combination of ASR and freezing and thawing. The concrete first developed ASR which produced microcracks and an avenue for additional water to enter the concrete. The water could not escape during rapid freezing and the pressure caused the microcracks to extend and expand. The cyclic applications of freezing and thawing allowed the cracking to extend to the present levels. Although reducing the moisture available to the alkali-silica gel will decrease the expansion, sealing larger cracks is required to prevent additional freezing and thawing distress. The magnitude of freezing and thawing expansion is apparent in Figure 3.8 and Figure 3.10. Between the beginning of monitoring and 91 days, the sections of moderate and severe damage expanded much more rapidly than in the summer months between 91 and 259 days. Again, between 259 days and one-year the expansion rate increased substantially. These two periods coincide with winter weather and freezing and thawing cycles, which shows that the expansion due to freezing and thawing is much more rapid than the expansion due to ASR. The ASR is also accelerated by warm weather and so much of the ASR damage occurs during the summer months.

4.3 Recommendations

From one-year of monitoring some preliminary recommendations are provided. Again, at least three years of monitoring are required to provide conclusive results from field testing of ASR mitigation. However, some preliminary recommendations are provided on changes to the application of treatments, the methods of mitigation, and the monitoring methods.

- All sections of minimal damage (and possibly moderate) should be treated with silane. Silane will reduce ASR related distress and microcracks. The formation of additional

microcracks must be prevented or freezing and thawing distress will rapidly exacerbate deterioration of the median barrier concrete.

- A single application of silane may not provide sufficient coverage, and the results from two applications of silane show the greatest reduction in expansion for sections of severe damage. A second application of silane should be applied within one year of applying the first application.
- The expansion joints between sections of moderate or severe damage have closed due to the expansions which have occurred in the median barrier. Therefore, additional slot cutting to reduce stresses may reduce crushing and spalling in some of the sections.
- Sealing cracks prior to treatment with either structural grade epoxy or an elastomeric sealant, which can expand and contract with the concrete, will reduce the ingress of moisture.
- A low viscosity injected epoxy applied to sections of moderate damage before treatment would improve the concrete strength and appearance, and reduce the ingress of moisture after treatment.
- Applying surface treatments during a period of low ambient humidity will minimize humidity trapped within the concrete
- Implementing a system of quality control will ensure proper application and sufficient dosage. The quality control should include penetration testing soon after application and additional testing after 5 years to measure the remaining useful life of the surface treatment.

- Developing an air tight relative humidity ports which provides a closed system and only allows equilibration between the concrete and air within the port is necessary for useful internal relative humidity monitoring.

5 References

ACI Committee 221. (1998). State-of-the-art report on alkali-aggregate reactivity (Report No. ACI 221.1R-98). American Concrete Institute, Farmington Hills, MI, 31 pp.

ASTM C1260-05. (2008a). Standard test method for potential alkali reactivity of aggregates (mortar-bar method). Annual Book of ASTM Standards 04.02, American Society for Testing and Materials (ASTM), West Conshohocken, Pennsylvania, 676-680.

ASTM C 1567-04. (2008b). Standard Test Method for Determining the Potential Alkali-Silica Reactivity of Combinations of Cementitious Materials and Aggregate (Accelerated Mortar-Bar Method). Annual Book of ASTM Standards 04.02, American Society for Testing and Materials (ASTM), West Conshohocken, Pennsylvania, 772-775.

ASTM C1293-08b. (2012). Standard test method for determination of length change of concrete due to alkali-silica reaction. Annual Book of ASTM Standards 04.02, American Society for Testing and Materials (ASTM), West Conshohocken, Pennsylvania, 687-686.

Bérubé, M.-A., Chouinard, D., Pigeon, M., Frenette, J., Rivest, M., & Vézina D., (2002a). Effectiveness of sealers in counteracting alkali–silica reaction in highway median barriers exposed to wetting and drying, freezing and thawing, and deicing salt. Canadian Journal of Civil Engineering, 29, 329-337.

Bérubé, M-A., Chouinard, D., Pigeon, M., Frenette, J., Boisvert, L., & Rivest, M. (2002b). Effectiveness of sealers in counteracting alkali–silica reaction in plain and air-entrained laboratory concretes exposed to wetting and drying, freezing and thawing, and salt water. Canadian Journal of Civil Engineering, 29, 289-300.

Construction Technology Laboratories Group (CTLGroup). (2012). Petrographic Examination of Concrete Specimens from I-540 Roadway and Barrier Wall (CTLGroup Project No. 157501). Skokie, Il. 16 pp.

Davies, G., & Oberholster, R. E. (1986). Use of the NBRI accelerated test to evaluate the effectiveness of mineral admixtures in preventing the alkali-silica reaction. Cement and Concrete Research, 17, 97-107.

Davies, G., & Oberholster, R. E. (1988). Alkali-silica reaction products and their development. Cement and Concrete Research, 18(4), 621-635.

Diamond, S. (1989). ASR—another look at mechanisms. Proceedings from 8th international Conference on Alkali-Aggregate Reaction (ICAAR). Kyoto, Japan, 83-94.

Drimalas, T., Folliard, K.J., Thomas, M.D.A., Fournier, B., & Bentivegna, A. (2012). Study of the effectiveness of lithium and silane treatments on field structures affected by ASR. Proceedings of the 14th International Conference on Alkali-Aggregate Reaction (ICAAR), Austin, Texas.

Duchesne, J., & Berube, M-A. (1994). The effectiveness of supplementary cementing materials in suppressing expansion due to ASR: Another look at the reaction mechanisms part 2: Pore solution chemistry. Cement and Concrete Research, 24(2), 221-230.

Du-you, L., Fournier, B., & Grattan-Bellew, P.E. (2004). A comparative study on accelerated test methods for determining alkali-silica reactivity of concrete aggregates. Proceedings of the 12th International Conference on Alkali-Aggregate Reaction (ICAAR), Beijing, China, 377-385.

Folliard, K. J., Barborak, R. C., Ideker, J. H., Fournier, B., & Thomas, M. D. A. (2007). Laboratory test methods for determining the dosage of lithium nitrate required to control ASR-induced expansion. Transportation Research Board (TRB) 86th Annual Meeting, Washington DC, 10 pp.

Folliard, K.J., Thomas, M.D.A., Fournier, B., Resendez, Y., Drimalas, T., & Bentivegna, A. (2012). Evaluation of mitigation measures applied to ASR-affected concrete elements: preliminary findings from Austin, TX Exposure Site. Proceeding of the 14th International Conference on Alkali Aggregate Reaction (ICAAR), Austin, Texas.

Fournier, B., & Bérubé, M.A. (2000). Alkali-Aggregate Reaction in Concrete: A Review of Basic Concepts and Engineering Implications. Canadian Journal of Civil Engineering, 27(2), 167-191.

Fournier, B., Bérubé, M.-A., & Frenette, J. (2000). Laboratory investigations for evaluating potential alkali-reactivity of aggregates and selecting preventive measures against alkali-aggregate reaction (AAR) - what do they really mean? Proceedings of the 11th International Conference on Alkali-Aggregate Reaction (ICAAR), Quebec, Canada, 287-296.

Fournier, B., Bérubé, M.A., Thomas, M.D.A., Smaoui, N. & Folliard, K.J. (2004). Evaluation and Management of Concrete Structures Affected by Alkali-Silica Reaction - A Review. MTL 2004-11 (OP). Natural Resources Canada. Ottawa (Canada), 59 pp.

Fournier, B., Bérubé, M-A., Folliard, K.J., & Thomas, M.D.A. (2010). Report on the Diagnosis, Prognosis, and Mitigation of Alkali- Silica Reaction (ASR) in Transportation Structures (Report No. FHWA-HIF-09-004). Federal Highway Administration, U.S. Department of Transportation, Washington DC, 154 pp.

Helmuth, R., Stark, D., Diamond, S., & Moranville-Regourd, M. (1993). Alkali-silica reactivity: an overview of research (Report No. SHRP-C-342). Strategic Highway Research Program (SHRP), National Research Council, Washington, DC, 105 pp.

Ideker, J.H., Bentivegna, A.F., Folliard, K.J., & Juenger, M.C.G. (2012a). Do current laboratory test methods accurately predict alkali-silica reactivity? ACI Materials Journal, 109(4), 395-402.

Ideker, J.H., Drimalas, T., Bentivegna, A.F., Folliard, K.J., Fournier, B., Thomas, M.D.A., Hooton, R.D., & Rogers, C.A., (2012b). The importance of outdoor exposure site testing. Proceeding of the 14th International Conference on Alkali Aggregate Reaction (ICAAR), Austin, Texas.

Johnston, D. P., Surdahl, R., & Stokes, D. B. (2000). A case study of a lithium-based treatment of an ASR-affected pavement. Proceedings of the 11th International Conference on Alkali-Aggregate Reaction (ICAAR), Quebec, Canada, 1149-1158.

Powers, T. C., & Steinour, H. H. (1955). An interpretation of some published researches on the Alkali-Aggregate Reaction, Part 1-the chemical reactions and mechanism of expansion. Journal of the American Concrete Institute, 26(6), 497-516.

Rogers, C.A., & Hooton, R.D. (1991). Reduction in mortar and concrete expansion with reactive aggregates due to alkali leaching. Cement, Concrete, and Aggregates, 13(1), 42-49.

Shehata, M.H., & Thomas, M.D.A. (2000). The effect of fly ash composition on the expansion of concrete due to alkali-silica reaction. Cement and Concrete Research, 30(7), 1063-1072.

Shrimer, F. (2000). Application and use of damage rating index in assessment of AAR-affected concrete-selected case studies. Proceeding of the 11th International Conference on Alkali Aggregate Reaction (ICAAR), Quebec, Canada, 899-907.

Smaoui, N., Berube, M. A., Fournier, B., Bissonnette, B., & Durand, B. (2004). Evaluation of the expansion attained to date by concrete affected by alkali-silica reaction. Part 1: Experimental study. Canadian Journal of Civil Engineering, 31(5), 826-845.

Stanton, T. E. (1940). Expansion of concrete through reaction between cement and aggregate. Proceedings American Society of Civil Engineers, 66(10), 1781-1811.

Stanton, T. E. (1943). Studies to develop an accelerated test procedure for the detection of adversely reactive cement-aggregate combinations. Proceedings of the American Society of Testing Materials (ASTM), 43, 875-893.

Stark, D. C. (1980). Alkali-silica reactivity: some reconsiderations. Cement, Concrete, and Aggregates, 2(2), 92-94.

Stark, D. (1990). The moisture condition of field concrete exhibiting alkali-silica reactivity. CANMET/ACI International Workshop on Alkali-Aggregate Reaction in Concrete, Halifax, Nova Scotia, 19 pp.

Stark, D. (1991). Handbook for the identification of alkali silica reactivity in highway structures (Report No. SHRP-C/FR-91-101). Strategic Highway Research Program, National Research Council, Washington, DC, 49 pp.

Stark, D. C., Morgan, B., Okamoto, P., & Diamond, S. (1993). Eliminating or minimizing alkali-silica reactivity (Report No. SHRP-C-343). Strategic Highway Research Program (SHRP), National Research Council, Washington, DC, 266 pp.

Stokes, D., Pappas, J., Thomas, M., & Folliard, K., (2002). Field cases involving treatment or repair of ASR affected concrete using lithium. Proceedings of the 6th CANMET/ACI International Conference on Durability of Concrete, Greece.

Swamy, R. N., & Al-Asali, M. M. (1988a). Engineering properties of concrete affected by alkali-silica reaction. ACI Materials Journal, 85(5), 367-374.

Swamy, R. N., & Al-Asali, M. M. (1988b). Expansion of concrete due to alkali-silica reaction. ACI Materials Journal, 85(1), 33-40.

Thomas, M. D. A. (1995). The role of fly ash and slag alkalis in alkali-silica reactions in concrete. CABNET/ACI International Workshop on Alkali-Aggregate Reactions in Concrete, Dartmouth, Nova Scotia, 181-204.

Thomas, M., Fournier, B., Folliard, K., Ideker, J., & Shehata, M. (2006a). Test methods for evaluating preventive measures for controlling expansion due to alkali–silica reaction in concrete. Cement and Concrete Research, 36(10), 1842-1856.

Thomas, T., Fournier, B., Folliard, K., Ideker, J., & Shehata M. (2006b). Test methods for evaluating preventive measures for controlling expansion due to alkali-silica reaction in concrete (Report No. ICAR 302-1). International Center for Aggregate Research (ICAR), Austin, Texas, 62 pp.

Thomas, M.D.A., Fournier, B., & Folliard, K.J., (2008). Report on determining the reactivity of concrete aggregates and selecting appropriate measures for preventing deleterious expansion in new concrete construction (Report No. FHWA-HIF-09-001). Federal Highway Administration, U.S. Department of Transportation, Washington, DC, 21 pp.

Thomas, M.D.A., Fournier, B., Folliard, K.J., & Resendez, Y.A. (2011). Alkali-silica reactivity field identification handbook (Report No. FHWA-HIF-12-022). Federal Highway Administration, U.S. Department of Transportation, Washington DC, 80 pp.

Thomas, M.D.A., Folliard, K.J., Fournier, B., Drimalas, T., & Rivard, P. (2012). Study of Remedial Actions on Highway Structures Affected by ASR. Proceedings of the 14th International Conference on Alkali-Aggregate Reaction (ICAAR), Austin, Texas.

Touma, W. E. (2000). Alkali-silica reaction in portland cement concrete: Testing procedures and mitigation methods. Proceedings of the 11th International Conference on Alkali-Aggregate Reaction (ICAAR), Quebec, 513-522.

Touma, W. E., Fowler, D. W., Carrasquillo, R. L., Folliard, K. J., & Nelson, N. R. (2001). Characterizing alkali-silica reactivity of aggregates using ASTM C 1293, ASTM C 1260, and their modifications (Paper No. 01-3019). Transportation Research Record: Journal of the Transportation Research Board, 1757, 157-165.

Tuan, C. Y., Kelly, M. T., Sun, H., & Buss, M. E. (2005). Evaluation of use of lithium nitrate in controlling alkali–silica reactivity in existing concrete pavement. Transportation Research Record: Journal of the Transportation Research Board, 1914, 34-44.

A1 Appendix A

A1.1 ASTM C1260 (AMBT) Data

Table A1.1. ASTM C1260 (AMBT) batch and expansion data.

Raw AMBT Data	Batch Data						Expansion Data (days)		
	W_{FA} (g)	W_W (g)	W_{CM} (g)	T_A (°F)	T_W (°F)	T_M (°F)	4	7	14
Van Buren, AR River sand 1	990.0	206.8	440.0	81.5	77.6	--	0.0112	0.1043	0.1995
Van Buren, AR River sand 2	990.2	206.8	440.0	81.1	79.1	85.6	0.0182	0.0623	0.1715
Van Buren, AR River sand 5	990.0	206.8	440.0	84.8	--	84.2	0.0218	0.0638	0.1523
Van Buren, AR River sand 6	990.0	206.8	440.0	84.8	--	84.2	0.0233	0.0647	0.1497
Pine Bluff, AR River sand 1	990.1	206.8	440.0	74.5	76.6	74.3	0.0383	0.0703	0.1800
Pine Bluff, AR River sand 2	989.9	206.8	440.0	72.6	74.7	70.3	0.0228	0.0718	0.1807
West Fork, AR limestone 1	989.8	206.8	440.0	74.5	80.1	--	0.0065	0.0062	0.0113
West Fork, AR limestone 2	989.8	206.8	440.0	87.3	76.7	--	0.0027	0.0058	0.0128
Springdale, AR Limestone 1	990.0	206.8	440.0	76.5	74.1	--	0.0075	0.0033	0.0117
Springdale, AR Limestone 2	989.9	206.8	440.0	86.2	74.3	82.5	0.0060	0.0080	0.0123
Granite Mountain, AR Granite 1	989.9	206.8	440.1	68.9	70.5	69	0.0030	0.0050	0.0025
Granite Mountain, AR Granite 2	989.9	206.9	440.0	68.9	74	69	0.0052	0.0063	0.0050
Muskogee, Ok River sand 1	990.0	206.8	440.0	77.4	75.9	76.5	0.0128	0.0323	0.0718
Muskogee, Ok River sand 2	990.0	206.8	440.0	77.4	75.9	76.5	0.0053	0.0208	0.0610

A1.2 ASTM C1293 (CPT) Data

Table A1.2. ASTM C1260 (AMBT) batch and expansion data.

Raw CPT Data	W_{FA} (lb)	W_{CA} (lb)	W_{W} (lb)	W_{CM} (lb)	W_{NaOH} (g)	Slump (in.)	Air Content (%)	Unit Weight (pcf)
Van Buren, AR River sand 1	85.50	132.10	24.30	52.40	205.70	3.00	1.70	149.56
Van Buren, AR River sand 2	87.10	134.00	20.80	52.40	221.06	3.00	1.70	149.56
Pine Bluff, AR River sand 1	85.50	132.20	24.30	52.40	221.10	3.50	1.90	148.47
Pine Bluff, AR River sand 2	85.50	132.20	24.30	52.40	221.10	2.75	1.60	149.08
Granite Mountain, AR Granite 1	87.72	128.34	24.52	52.44	221.00	7.25	1.20	148.59
Granite Mountain, AR Granite 2	87.72	128.34	24.52	52.44	221.00	7.50	1.20	148.59
Dover, OK River sand 1	85.37	130.68	24.52	52.44	221.00	5.50	1.20	149.16
Dover, OK River sand 2	85.37	130.68	24.52	52.44	221.00	5.25	1.50	147.99
Jobe, TX Sand 1	85.37	130.68	24.52	52.44	221.00	3.50	1.60	147.99
Jobe, TX Sand 2	85.37	130.68	24.52	52.44	221.00	4.00	1.40	148.31
Muskogee, OK River sand 1	86.61	130.68	23.44	52.44	221.00	7.50	0.90	148.55
Muskogee, OK River sand 2	86.61	130.68	23.44	52.44	221.00	8.50	1.00	146.83
West Fork, AR Limestone 1	85.37	131.99	24.52	52.44	221.10	5.50	2.50	146.31

A1.3 Strain Rate Data from Median Barriers

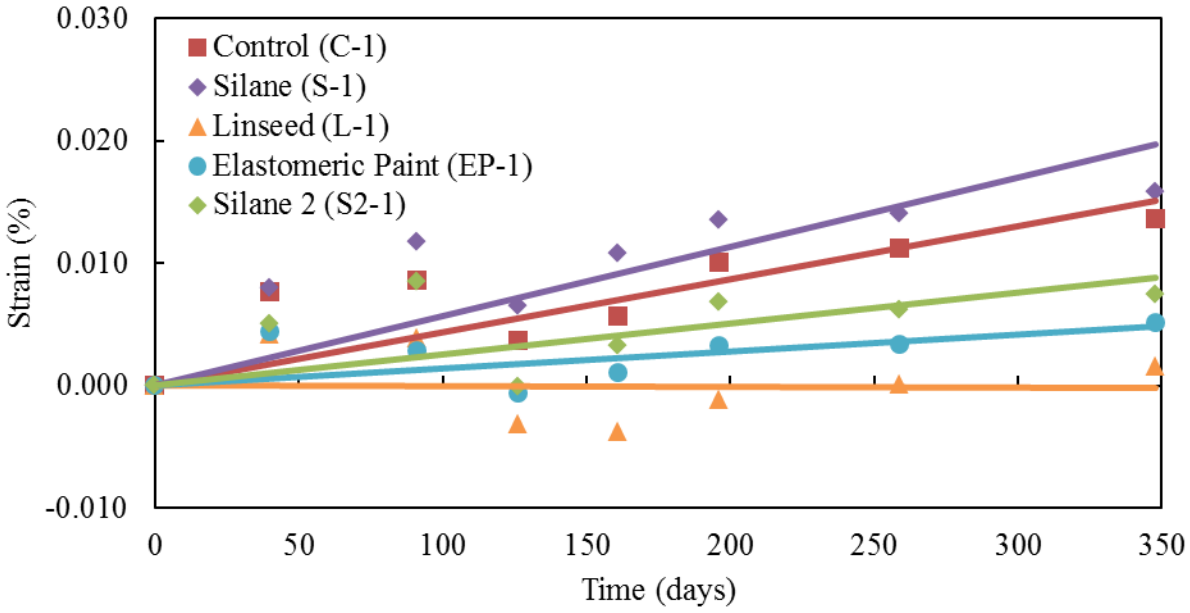

Figure A1.1. Temperature normalized vertical strain (%) with respect to time (days) strain rate results for median barrier sections which exhibit minimal damage.

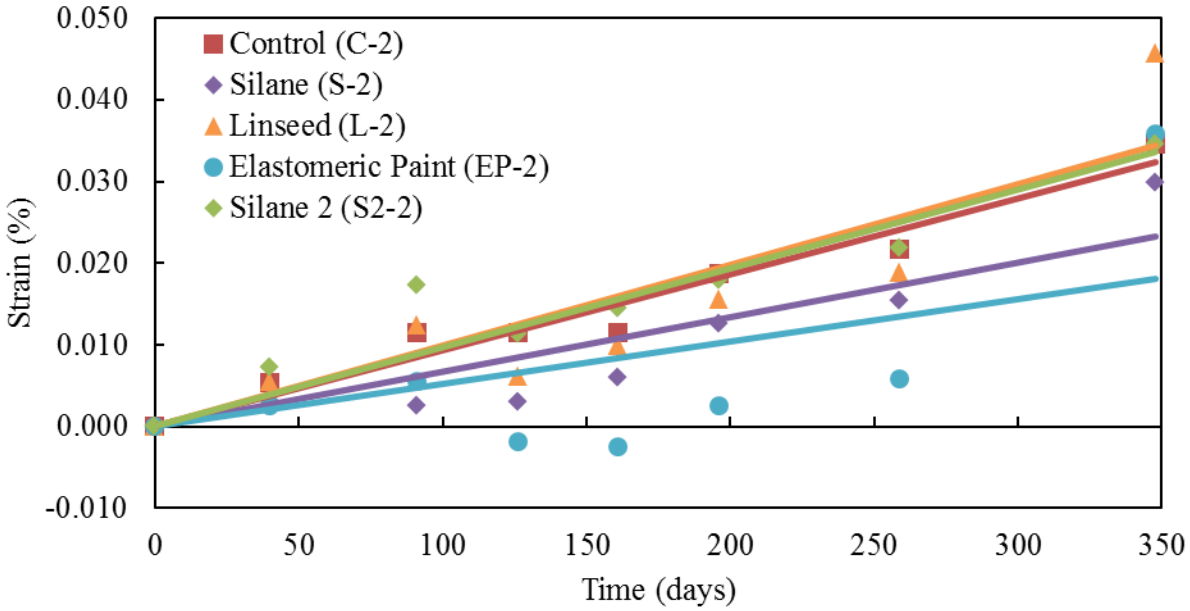

Figure A1.2. Temperature normalized vertical strain (%) with respect to time (days) strain rate results for median barrier sections which exhibit moderate damage.

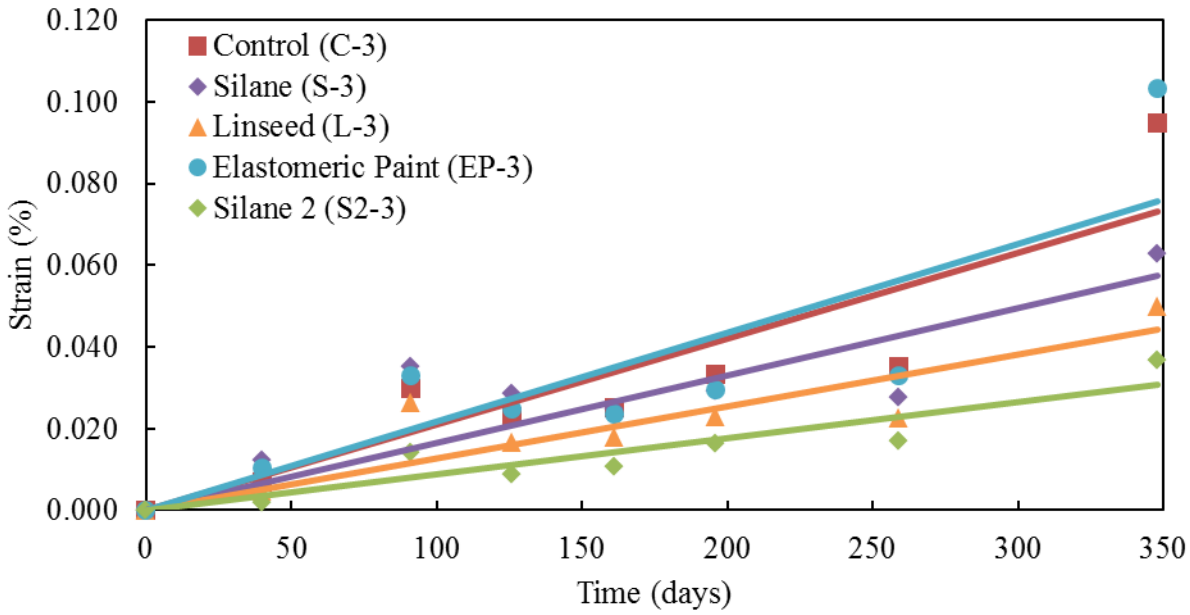

Figure A1.3. Temperature normalized vertical strain (%) with respect to time (days) strain rate results for median barrier sections which exhibit severe damage.

A1.4 Raw Strain Data from Median Barriers

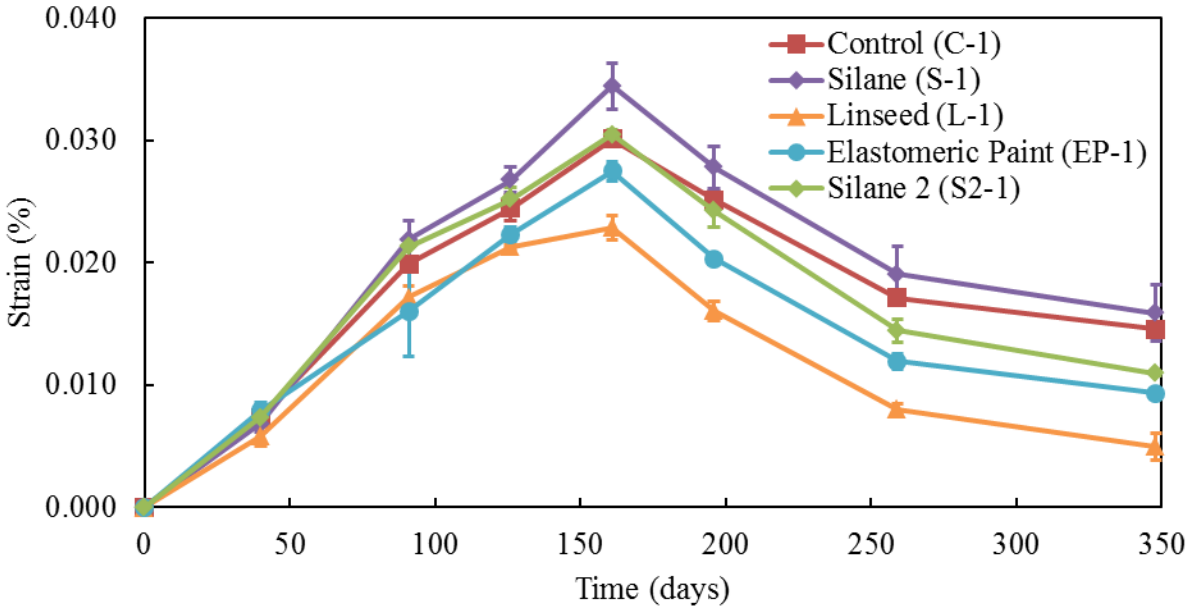

Figure A1.4. Raw vertical strain (%) with respect to time (days) results for median barrier sections which exhibit minimal damage. Error bars represent standard error between two sides of length-change grid.

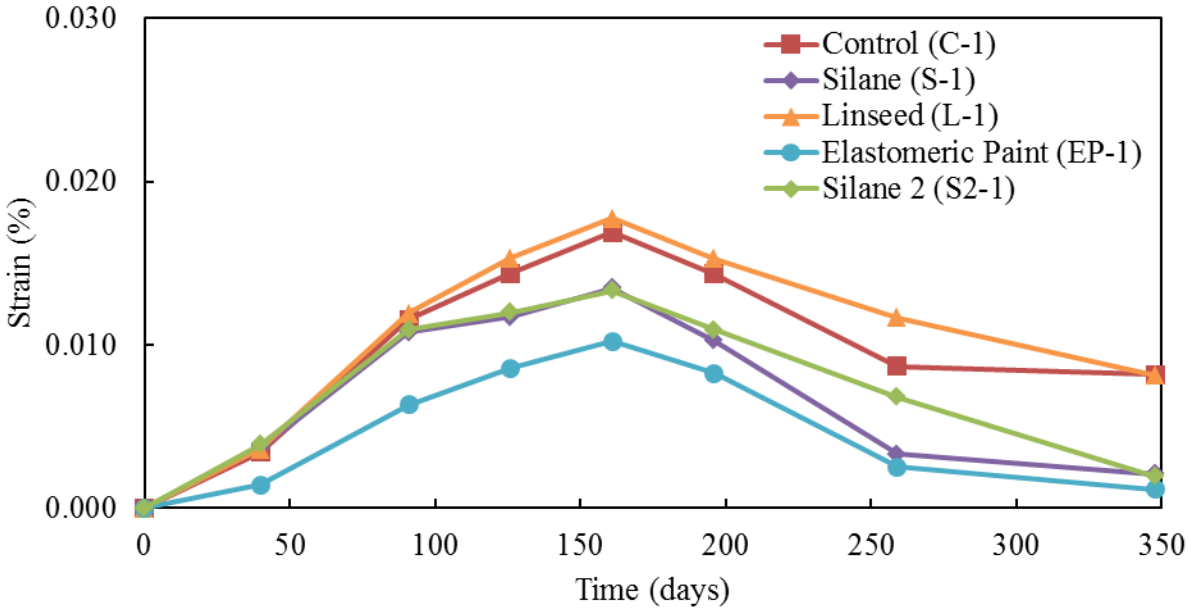

Figure A1.5. Raw longitudinal strain (%) with respect to time (days) results for median barrier sections which exhibit minimal damage.

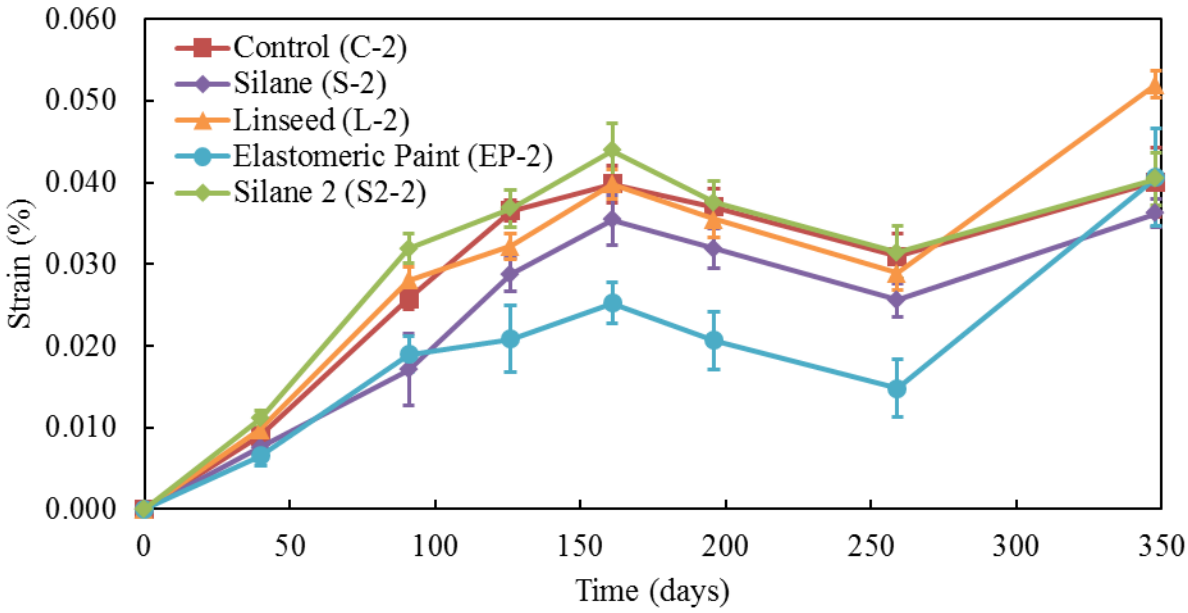

Figure A1.6. Raw vertical strain (%) with respect to time (days) results for median barrier sections which exhibit moderate damage.

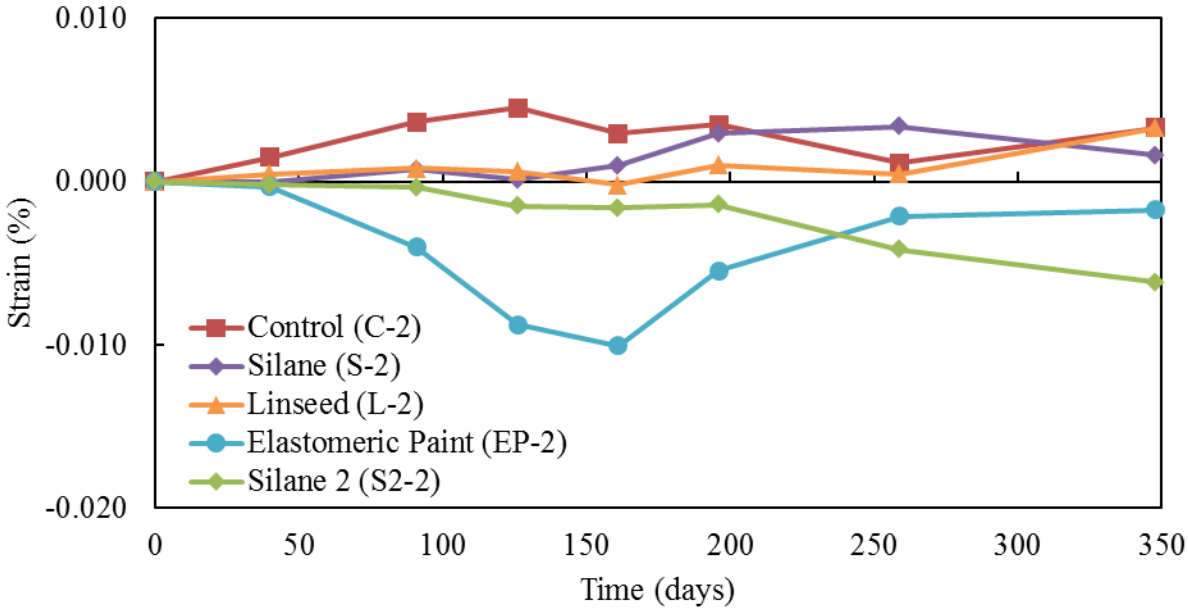

Figure A1.7. Raw longitudinal strain (%) with respect to time (days) results for median barrier sections which exhibit moderate damage.

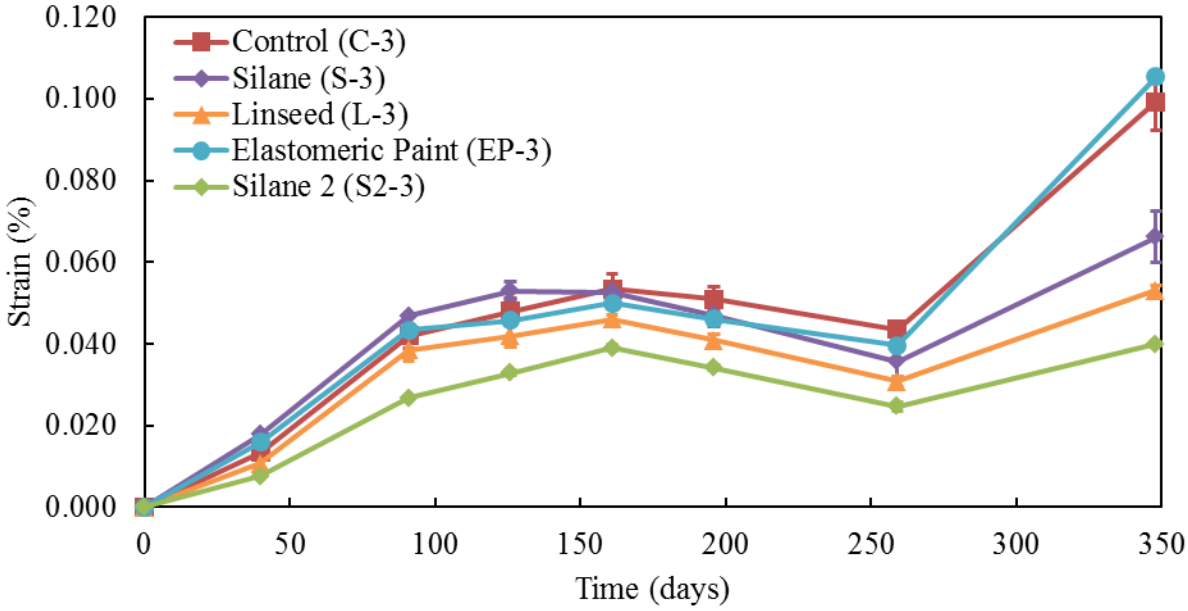

Figure A1.8. Raw vertical strain (%) with respect to time (days) results for median barrier sections which exhibit severe damage.

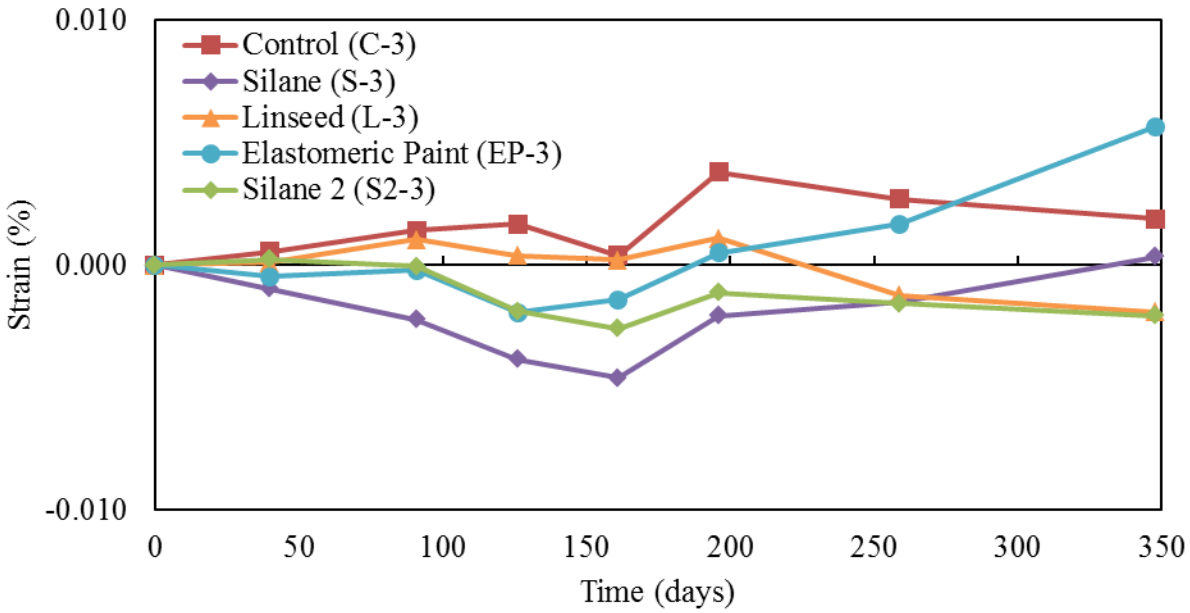

Figure A1.9. Raw longitudinal strain (%) with respect to time (days) results for median barrier sections which exhibit severe damage.